supernatants were collected and determined for protein content using the Bradford method (Bio-Rad Laboratories, Hercules, CA). Proteins (40 μg) were resolved under denaturing conditions by 10% sodium dodecyl sulfate-polyacrylamide gel electrophoresis (SDS-PAGE) and transferred onto nitrocellulose membranes (Bio-Rad). The transferred membranes were blocked for 1 hr in 5% nonfat dry milk in TBST (25 mmol/L Tris-HCl, pH 7.4, 125 mmol/L NaCl, 0.05% Tween 20) and incubated with the appropriate primary antibodies at 4°C for 10 hr. Membranes were washed twice with TBST for 10 min and incubated with horseradish peroxidase-coupled isotype-specific secondary antibodies for 1 hr at room temperature. The immune complexes were detected by enhanced chemiluminescence detection system (Amersham Biosciences, Piscataway, NJ) and quantified using analyst/PC densitometry software (Bio-Rad). Mean densitometry data from independent experiments were normalized to result in cells in the control. The data were presented as the mean ± SD and analyzed by Student's *t* test.

Immunoprecipitation

After the indicated treatments, cells were washed with ice-cold phosphate-buffered saline and lysed in lysis buffer at 4°C for 20 min. After centrifugation at 14,000 × *g* for 15 min at 4°C, the supernatants were collected and determined for protein content using the Bradford method (Bio-Rad Laboratories, Hercules, CA). Lysates were normalized, and 60 μg proteins were incubated with anti-Bcl-2 antibodies for 14 hr at 4°C followed by incubation with protein A-conjugated Sepharose. The immune complexes were washed with 20 vols. of lysis buffer, resuspended in 2× Laemmli sample buffer, and boiled at 95°C for 5 min. Immune complexes were separated by 10% SDS-PAGE and analyzed by Western blotting as described.

RESULTS

Curcumin enhances cisplatin-induced apoptosis in H460 cells

To investigate the role of curcumin in cisplatin-induced apoptosis, we first evaluated the dose-dependent effect of cisplatin on apoptotic cell death in human non-small cell lung cancer H460 cells in the presence or absence of curcumin. Cells were treated with various concentrations of cisplatin (0–250 μmol/L) and apoptosis was determined after 24 hr by Hoechst 33342 nuclear staining assay. Cisplatin treatment caused a dose-dependent increase in apoptotic cell death as compared to nontreated control (Figure 1(a)). Apoptotic cells exhibited intense nuclear fluorescence, chromatin condensation and/or fragmentation, characteristic of apoptosis. At the treatment dose of 50 μmol/L, approximately 10% of the treated cells showed apoptotic nuclear morphology with the cell death response exceeding 43% at the treatment dose of 250 μmol/L. To confirm the apoptosis-inducing effect of cisplatin in these cells, cells were similarly treated with cisplatin and cell viability was determined by MTT assay. Figure 1(b) shows that cisplatin was able to decrease cell viability in a dose-dependent manner, consistent with the apoptosis results.

To investigate the role of curcumin in the regulation of cisplatin-induced apoptosis, cells were pretreated with various concentrations of curcumin (0–100 μmol/L) and then treated with the apoptotic dose of cisplatin (100 μmol/L). The results showed that curcumin significantly increased the apoptotic effect of cisplatin, whereas curcumin alone, when used at low concentrations (0–50 μmol/L), had minimal apoptotic effect on the cells (Figure 1(c)). At high doses (100 μmol/L), however, curcumin induced significant apoptosis (∼10%). These results indicate that curcumin enhances apoptotic cell death of cisplatin and can directly induce apoptosis when used at high doses. To confirm the sensitizing effect of curcumin, cells were similarly treated with cisplatin and curcumin, and their viability was determined by MTT assay. Consistent with the Hoechst apoptosis assay, curcumin further decreased cell viability in response to cisplatin treatment (Figure 1(d)). Curcumin alone induced minimal cytotoxic effect except at the high concentration of 100 μmol/L.

Because previous studies have shown that curcumin can induce intracellular reactive oxygen species (ROS) generation and increased ROS has been linked to apoptotic cell death (25–29), we investigated whether the sensitizing effect of curcumin was associated with its ROS-inducing activity. Figures 1(c) and (d) show that addition of a general antioxidant, *N*-acetyl cysteine (NAC), potently inhibited the apoptotic sensitizing effect of curcumin, suggesting that ROS was involved in this apoptotic sensitization. It is worthy to note that co-treatment of the cells with pan-caspase inhibitor zVAD-fmk completely inhibited the apoptotic effect of both curcumin and cisplatin, indicating the requirement of caspase activation in the cell death response.

Curcumin induces intracellular ROS generation in H460 cells

To provide supporting evidence for the role of ROS in the apoptosis-enhancing effect of curcumin, we analyzed ROS generation in cells treated with various concentrations of curcumin in the presence or absence of NAC. Flow cytometric analysis of ROS generation using DCF-DA as a fluorescent probe shows that curcumin was able to induce ROS generation in a dose-dependent manner and this effect was inhibited by the antioxidant NAC (Figure 2(a)). Cisplatin can also induce ROS generation and this effect can be enhanced by the addition of curcumin (Figure 2(b)). These data suggest that curcumin acts as a prooxidant and promotes the ROS-inducing and apoptosis-inducing effects of cisplatin. To determine specific ROS induced by curcumin, cells were treated with the agent in the presence or absence of various known specific antioxidants, including MnTBAP (a superoxide dismutase mimetic and scavenger of superoxide anion), catalase (hydrogen peroxide scavenger), and sodium formate (hydroxyl radical scavenger). Cells were then analyzed for ROS as described. The results show that MnTBAP significantly inhibited

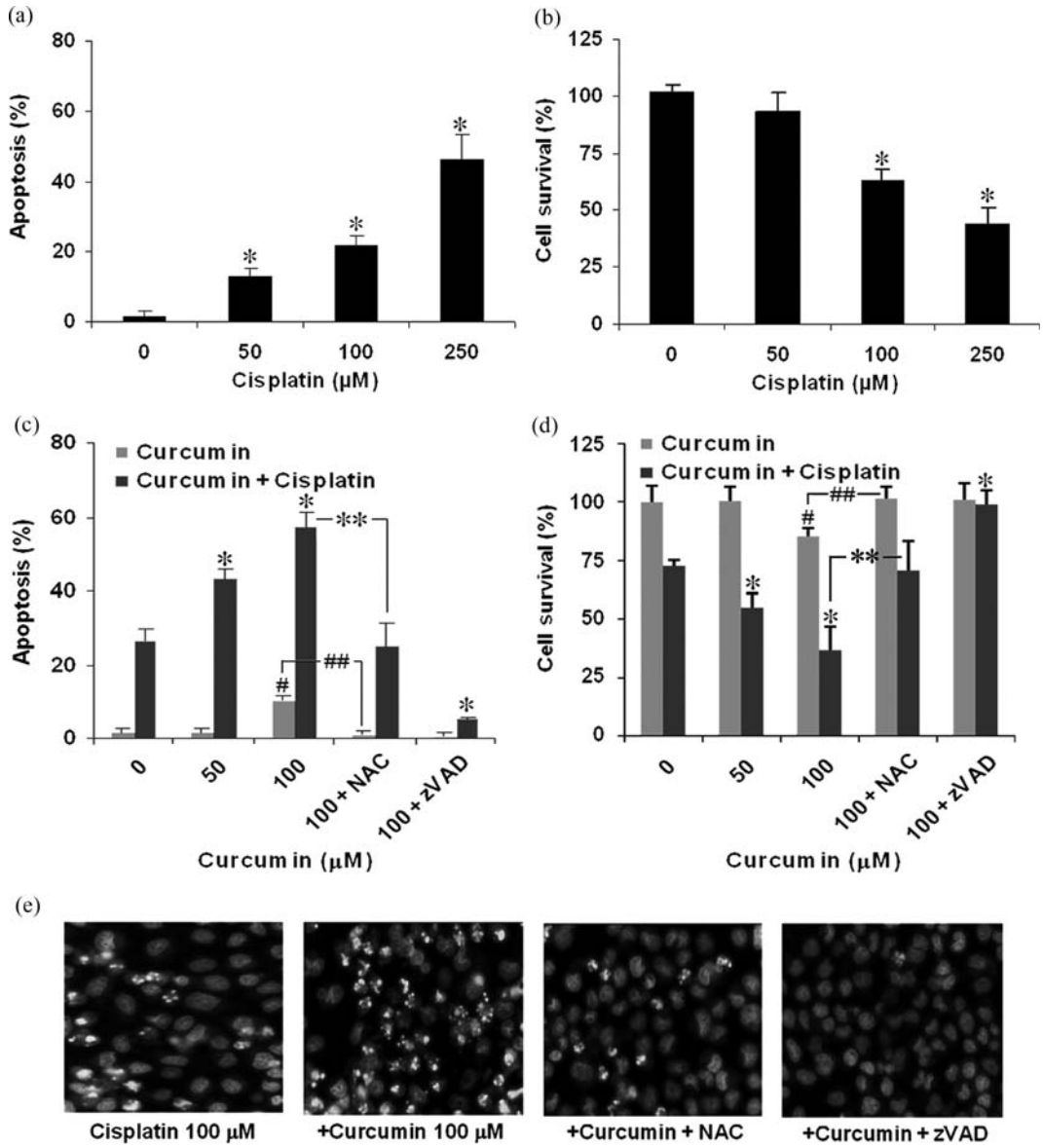

Figure 1. Cisplatin induces cell apoptosis and its sensitization by curcumin. H460 cells were treated with various concentrations of cisplatin (0–250 μmol/L) for 24 hr. (a) Effect of cisplatin treatment on cell apoptosis determined by Hoechst 33342 assay. (b) Effect of cisplatin on cell viability analyzed by MTT assay. (c) Effect of curcumin treatment alone and in combination with cisplatin on cell apoptosis in the presence or absence of antioxidant NAC or caspase inhibitor zVAD-fmk. Cells were pretreated with NAC (5 mmol/L), zVAD-fmk (10 μmol/L), or curcumin (0–100 μmol/L) for 30 min, after which they were treated, or left untreated, with cisplatin (100 μmol/L) for 24 hr. Apoptosis was then determined by Hoechst 33342 assay. (d) Effect of curcumin treatment alone or in combination with cisplatin on cell survival in the presence or absence of antioxidant NAC or caspase inhibitor zVAD-fmk. After specific treatments, cell survival was determined by MTT assay. (e) Morphology of apoptotic nuclei in cells treated with cisplatin (100 μmol/L) with or without curcumin (100 μmol/L), NAC, or zVAD-fmk, as determined by fluorescence microscopy of Hoechst-stained cells. Values are means $\pm$ SD ($n = 3$). * and #, $p < 0.05$ versus non-treated control; **, $p < 0.05$ versus cisplatin (100 μmol/L) and curcumin (100 μmol/L)-treated controls; ##, $p < 0.05$ versus curcumin (100 μmol/L)-treated control.

curcumin-induced ROS generation, whereas other antioxidants had no significant effect (Figure 2(c)). These findings indicate that superoxide anion is a major ROS induced by curcumin in the treated cells. Studies using dihydroethidium (DHE) as a fluorescent probe for superoxide anion confirmed this result (data not shown).

Curcumin promotes down-regulation of Bcl-2 by cisplatin through an ROS-dependent mechanism

Bcl-2 is a major anti-apoptotic protein of the mitochondrial death pathway known to be involved in the regulation of

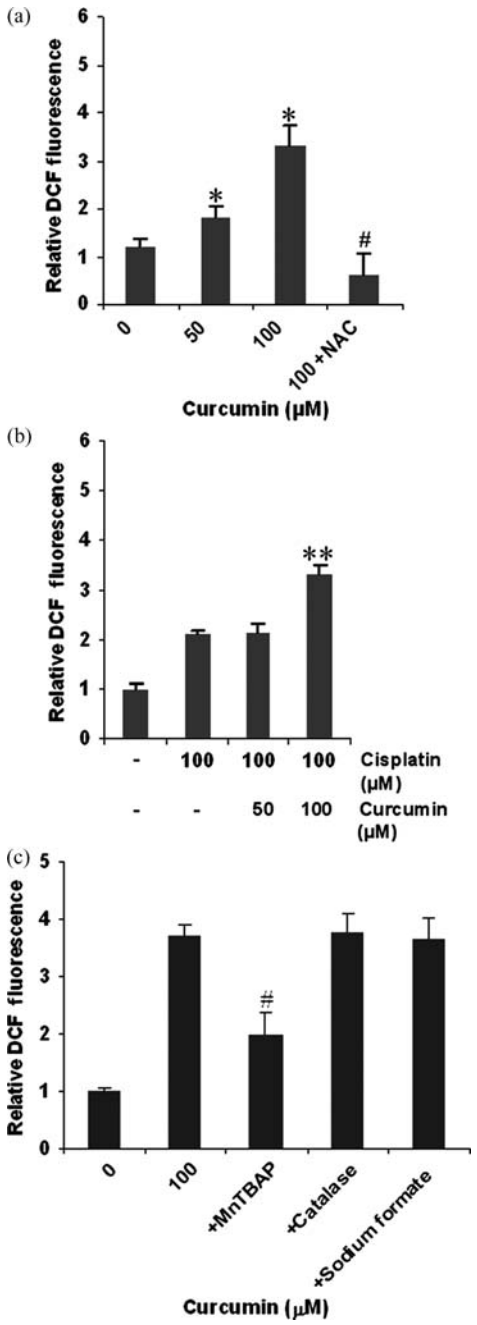

Figure 2. Effect of cisplatin and curcumin on intracellular ROS generations. (a) H460 cells were treated with curcumin (0–100 μmol/L) in the presence or absence of NAC (5 mmol/L) for 1 hr. Cellular ROS levels were then measured by flow cytometry using DCF-DA as a fluorescent probe, as described under Materials and Methods. (b) Cells were treated with cisplatin (0–100 μmol/L) or co-treated with cisplatin (100 μmol/L) and curcumin (0–100 μmol/L). (c) Cells were pre-treated with MnTBAP (100 μmol/L), catalase (1,000 U/ml), or sodium formate (5 mmol/L) for 30 min, and then treated with curcumin (100 μmol/L) for 1 hr. Values are means $\pm$ SD ($n = 4$). *, $p < 0.05$ versus non-treated control; **, $p < 0.05$ versus cisplatin-treated control; #, $p < 0.05$ versus curcumin (100 μmol/L)-treated control.

apoptotic cell death induced by cisplatin (30–33). Overexpression of Bcl-2 has also been associated with cisplatin resistance in many cell types (10–14). To test whether curcumin might promote cisplatin-induced cell death through down-regulation of Bcl-2, we analyzed Bcl-2 expression levels in cells treated with curcumin and cisplatin by Western blotting. Figures 3(a) and (b) show that cisplatin treatment caused a significant reduction in Bcl-2 expression which was blocked by the addition of NAC, indicating that cisplatin-induced Bcl-2 down-regulation was mediated through an ROS-dependent mechanism. Importantly, addition of curcumin enhanced the Bcl-2 down-regulating effect of cisplatin (Figure 3(c) and (d)). Co-treatment of the cells with NAC inhibited this down-regulation, supporting the role of ROS in Bcl-2 down-regulation induced by cisplatin and curcumin.

Superoxide-mediated down-regulation of Bcl-2 by curcumin

Curcumin was earlier shown to promote Bcl-2 down-regulation by cisplatin in an ROS-dependent manner. We next determined whether curcumin can directly induce Bcl-2 down-regulation and, if so, what specific ROS are involved. Cells were treated with various concentrations of curcumin and its effect on Bcl-2 expression was determined by Western blotting. The result shows that curcumin could directly induce Bcl-2 down-regulation in dose-dependent manner and that this effect was inhibited by the antioxidant NAC (Figure 3(e)). To determine the specific ROS involved, cells were treated with curcumin in the presence or absence of specific ROS scavengers, including MnTBAP, catalase, deferoxamine, and sodium formate; and their effect on Bcl-2 expression was determined. Figures 4(a) and (b) show that the superoxide anion scavenger MnTBAP completely inhibited curcumin-induced Bcl-2 down-regulation, whereas other antioxidants had no significant inhibitory effect. These results indicate that superoxide anion is the primary ROS responsible for the down-regulating effect of curcumin on Bcl-2.

Curcumin induces Bcl-2 down-regulation via proteasomal degradation

Since the previous studies have shown that Bcl-2 is down-regulated primarily through the proteasomal degradation pathway (14, 34, 35), we tested whether such degradation is involved in curcumin-induced Bcl-2 down-regulation. Cells were treated with curcumin in the presence or absence of lactacystin (LAC), a specific proteasome inhibitor, and its effect on Bcl-2 expression was examined. Figures 5(a) and (b) show that LAC completely inhibited the down-regulation of Bcl-2 by curcumin, indicating that this down-regulation was mediated through proteasomal degradation. This result was confirmed by using another proteasome inhibitor, MG132, which showed a similar inhibitory effect on curcumin-induced Bcl-2 down-regulation. To test whether Bcl-2 down-regulation may be mediated through lysosomal degradation, a known inhibitor of lysosomal

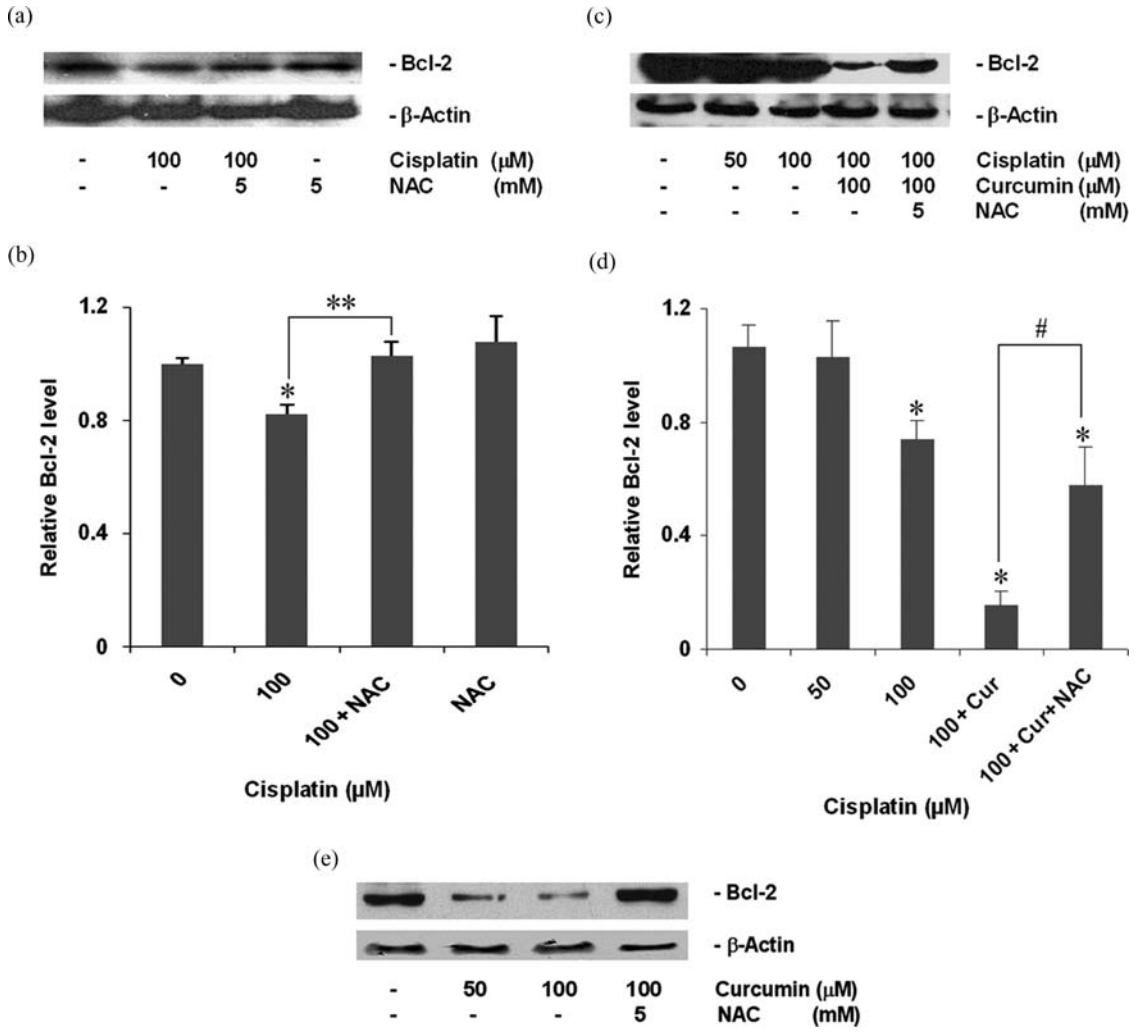

Figure 3. Curcumin enhances cisplatin-induced Bcl-2 down-regulation. (a) H460 cells were treated with cisplatin (100 μmol/L) in the presence or absence of NAC (5 mmol/L) for 24 hr. Bcl-2 expression levels were then determined by Western blotting. Blots were reprobed with β-actin antibody to confirm equal loading of samples. (b) The Western blot signals were quantified by densitometry and mean data from independent experiments were normalized to the result obtained in non-treated control cells. Values represent means $\pm$ SD ($n = 3$). *, $p < 0.05$ versus non-treated control; **, $p < 0.05$ versus cisplatin-treated control. (c) Cells were treated with cisplatin (0–100 μmol/L) or co-treated with cisplatin (100 μmol/L) and curcumin (100 μmol/L) in the presence or absence of NAC (5 mmol/L) for 24 hr. Bcl-2 levels were determined using Western blotting. (d) Densitometry was performed to determine the relative levels of Bcl-2. Values represent means $\pm$ SD ($n = 3$). *, $p < 0.05$ versus non-treated control; #, $p < 0.05$ versus cisplatin and curcumin-treated control. (e) H460 cells were treated with curcumin (0–100 μmol/L) in the presence or absence of NAC (5 mmol/L) for 24 hr and Bcl-2 expression was determined by Western blotting.

degradation, concanamycin A (CMA) (36), was used. Figure 5(b) shows that CMA had minimal effect on curcumin-induced Bcl-2 down-regulation. A similar pattern of Bcl-2 alterations was also observed in cells co-treated with cisplatin and curcumin in the presence or absence of proteasome and lysosome inhibitors (Figure 5(c) and (d)). Together, these results indicate that proteasomal degradation is the primary mechanism of Bcl-2 down-regulation induced by curcumin and cisplatin.

To further investigate the mechanism by which curcumin induced Bcl-2 down-regulation, we analyzed ubiquitination of Bcl-2 in response to curcumin treatment by immunoprecipitation. After treatment with curcumin, cell lysates were prepared and immunoprecipitated using anti-Bcl-2 antibody. The resulting immune complexes were then analyzed for ubiquitin by Western blotting. The results show that curcumin was able to induce Bcl-2 ubiquitination in a time-dependent manner (Figure 5(e) and (f)), as indicated by the increased formation of ubiquitin-Bcl-2 complexes. These results along with our earlier proteasome inhibition studies indicate that curcumin induced Bcl-2 down-regulation via the ubiquitin-proteasomal degradation pathway.

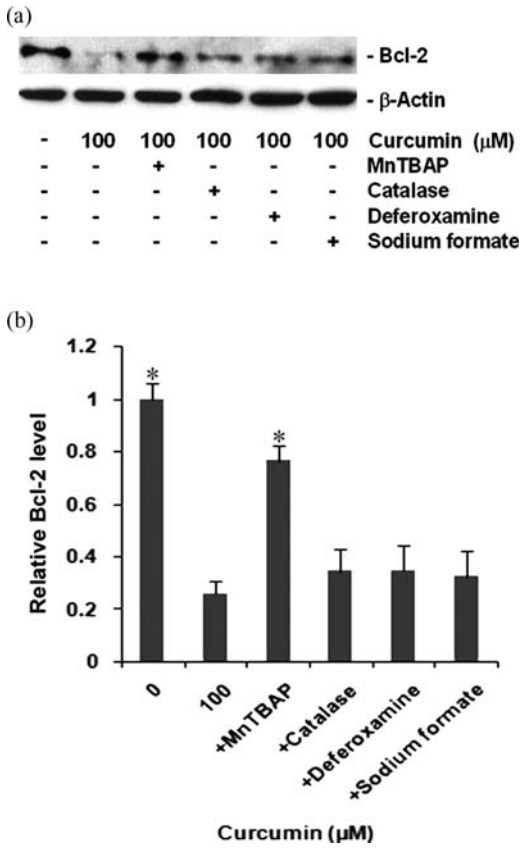

Figure 4. Effect of ROS scavengers on curcumin-induced Bcl-2 down-regulation. (a) H460 cells were pre-treated with MnTBAP (100 μmol/L), catalase (1,000 U/ml), deferoxamine (20 mmol/L), or sodium formate (5 mmol/L) for 30 min and then treated with curcumin (100 μmol/L) for 24 hr. Bcl-2 expression levels were determined by Western blot analysis. (b) Bcl-2 expression levels were shown as means $\pm$ SD ($n = 3$). *, $p < 0.05$ versus curcumin-treated control.

Curcumin reverses cisplatin resistance in Bcl-2 overexpressing cells

The essential role of Bcl-2 in apoptosisregulation in the treated cells was further demonstrated by the observation that ectopic expression of Bcl-2 by gene transfection conferred resistance to cisplatin-induced cell death as compared to control transfection (Figure 6(a) and (b)). Western blot analysis of Bcl-2 expression in the transfected cells shows an increase in the protein level in Bcl-2-transfected cells but not in mock-transfected cells (Figure 6(c)). These results indicate the role of Bcl-2 in cisplatin death resistance in the test cell system.

Having demonstrated the effect of Bcl-2 on apoptosis regulation, we next tested the potential sensitization effect of curcumin in cisplatin-resistant Bcl-2 overexpressing cells. Lung epithelial H460 cells overexpressing ectopic Bcl-2 were exposed to various concentrations of cisplatin in the presence or absence of curcumin (100 μmol/L), and 24 hr after the treatment, cells were analyzed for viability using MTT assay. Figure 6(d) shows that co-treatment of the cells with cisplatin and curcumin significantly reduced cell viability as compared to control treatment with cisplatin alone, indicating that curcumin was able to overcome cisplatin resistance in these cells. Our results also show that increased expression of Bcl-2 in the overexpressing cells was responsible for cisplatin resistance and that curcumin was able to decrease Bcl-2 expression similar to that observed in normal H460 cells (Figure 6(e) and (f)). Together, these results indicate that curcumin can increase the sensitivity of cells to cisplatin-induced cell death through Bcl-2 down-regulation.

DISCUSSION

We reported herein that curcumin can be used to sensitize human lung epithelial cancer cells to cisplatin-induced apoptosis. The potentiation effect of curcumin on cancer cell death induced by a variety of chemotherapeutic agents has previously been described by several groups. Jung *et al*. (37) and Deeb *et al*. (38) reported the sensitizing effect of curcumin on tumor necrosis factor-related apoptosis-inducing ligand (TRAIL)-induced apoptosis of renal cancer and prostate cancer cells, while Notarbartolo *et al*. (27) showed increased growth-inhibitory effect of doxorubicin and cisplatin by curcumin in hepatic cancer cells. Weir *et al*. (39) reported curcumin-induced cell cycle arrest and apoptosis in chemoresistant ovarian cancer cells. In combination with cisplatin, curcumin exerted its anticancer activity through the inhibition of Akt and the activation of p38 MAPK (39). Moreover, the alteration in NF-κB signaling pathway was shown to be associated with curcumin and cisplatin synergistic cytotoxicity (27). However, the effect of this combined use on Bcl-2 protein has not been well investigated. Since resistance to apoptosis is a key characteristic of cancer cells, the results of these studies suggest that curcumin could potentially be used as a chemotherapeutic sensitizing agent in various forms of cancer.

Several mechanisms of chemosensitization of curcumin have been proposed, including inactivation of NF-κB through IκBα dephosphorylation, modulation of Akt and p38, and up-regulation of death receptor 5 (DR5) (37, 38, 40, 41). Studies have also shown that ROS is a key mediator of apoptosis sensitization of curcumin (42); however, the precise role and mechanism of apoptosis sensitization are unclear. Up-regulation and accumulation of ROS have been associated with mitochondrial membrane potential disruption, and consequently the imbalance between the pro- and anti-apoptotic signals. Bcl-2 is a key anti-apoptotic protein of the mitochondrial pathway whose dysregulation results in cytochrome c release and subsequent activation of caspase cascade leading to apoptosis (42).

Cisplatin, a widely used cancer chemotherapeutic agent, has been long known to induce apoptosis through the mitochondrial death pathway. Mode of action of cisplatin has been shown to be associated with its ability to generate ROS as well as interact with DNA (43), which subsequently impairs the balance of Bcl-2 family members. Down-regulation of anti-apoptotic members, especially Bcl-2, has been widely regarded

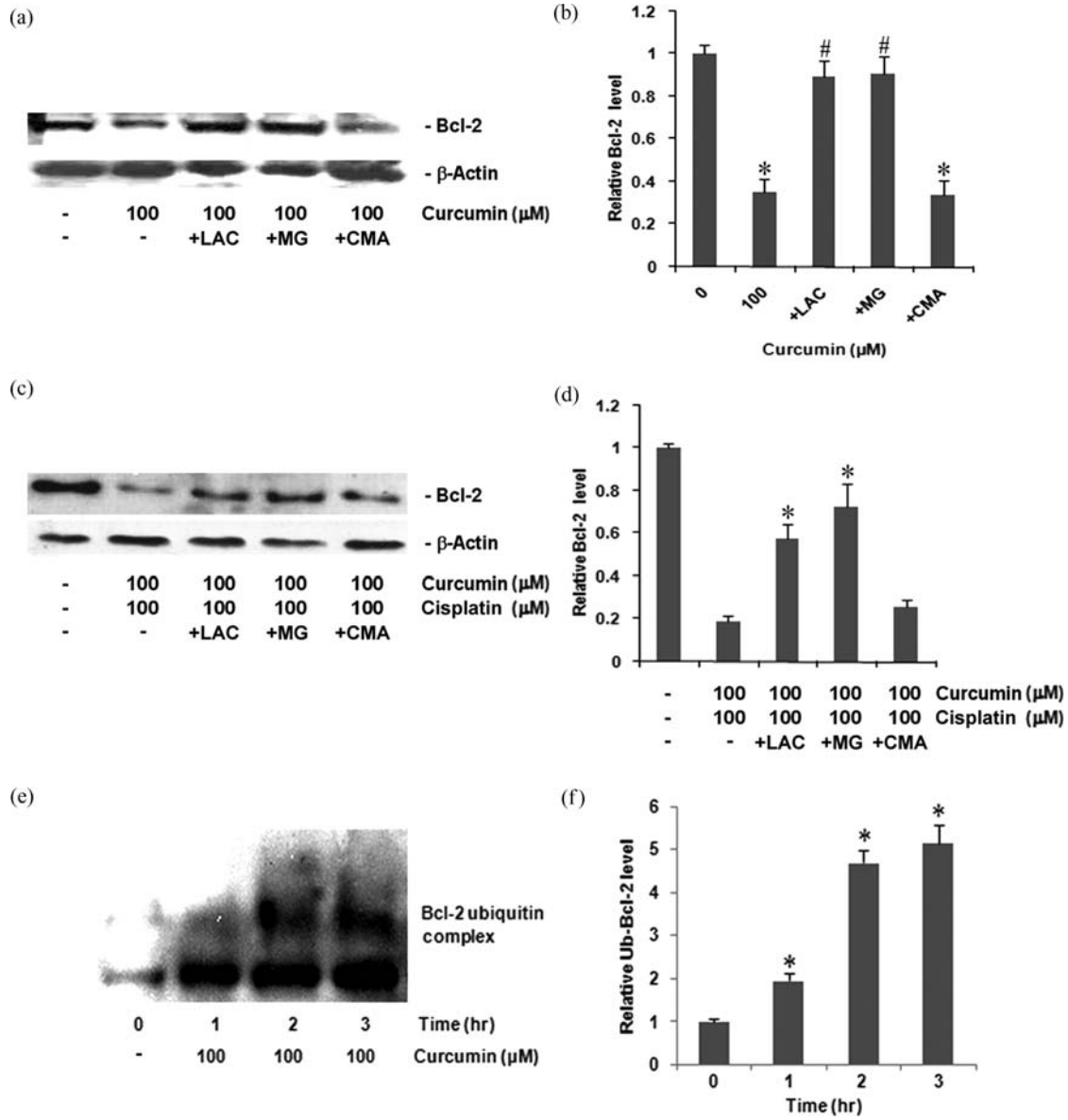

Figure 5. Curcumin induces Bcl-2 down-regulation via ubiquitin-proteasomal degradation pathway. (a) H460 cells were pretreated with proteasome inhibitor LAC (10 μmol/L) or MG132 (10 μmol/L), or with lysosome inhibitor CMA (1 μmol/L), for 1 hr and then treated with curcumin (100 μmol/L) for 24 hr. The expression levels of Bcl-2 were determined by Western blot analysis. (b) The immune complexes were quantified by densitometry and mean data from independent experiments were normalized to the result obtained in curcumin-treated control cells. Values are means $\pm$ SD ($n = 3$). *, $p < 0.05$ versus non-treated control; #, $p < 0.05$ versus curcumin-treated control. (c) Cells were pretreated with proteasome or lysosome inhibitors as described above and then treated with cisplatin (100 μmol/L) and curcumin (100 μmol/L). After 24 hr, Bcl-2 levels were determined by Western blot analysis. (d) Densitometric analysis of Bcl-2 levels. Values are means $\pm$ SD ($n = 3$). *, $p < 0.05$ versus non-treated control. (e) H460 cells were pretreated with proteasome inhibitor LAC (10 μmol/L) for 1 hr, and then treated with curcumin (100 μmol/L) for several times as indicated. Cell lysates were immunoprecipitated with anti-Bcl-2 antibody, and the immune complexes were analyzed for ubiquitin by Western blotting. (f) Densitometry was performed to determine the relative levels of Bcl-2 ubiquitin complexes. Values are means $\pm$ SD ($n = 3$). *, $p < 0.05$ versus non-treated control.

as a key initial step of apoptosis signaling via the mitochondrial death pathway (44). Bcl-2 expression has also been associated with favorable clinical and pathological characteristics and prognosis of several human cancers including NSCLC (45). Moreover, amplification or overexpression of Bcl-2 has been linked to cancer chemoresistance, particularly to cisplatin (46).

We have shown in the present study that curcumin increased cell sensitivity to cisplatin-induced apoptosis through a mechanism that involves ROS generation and Bcl-2 down-regulation.

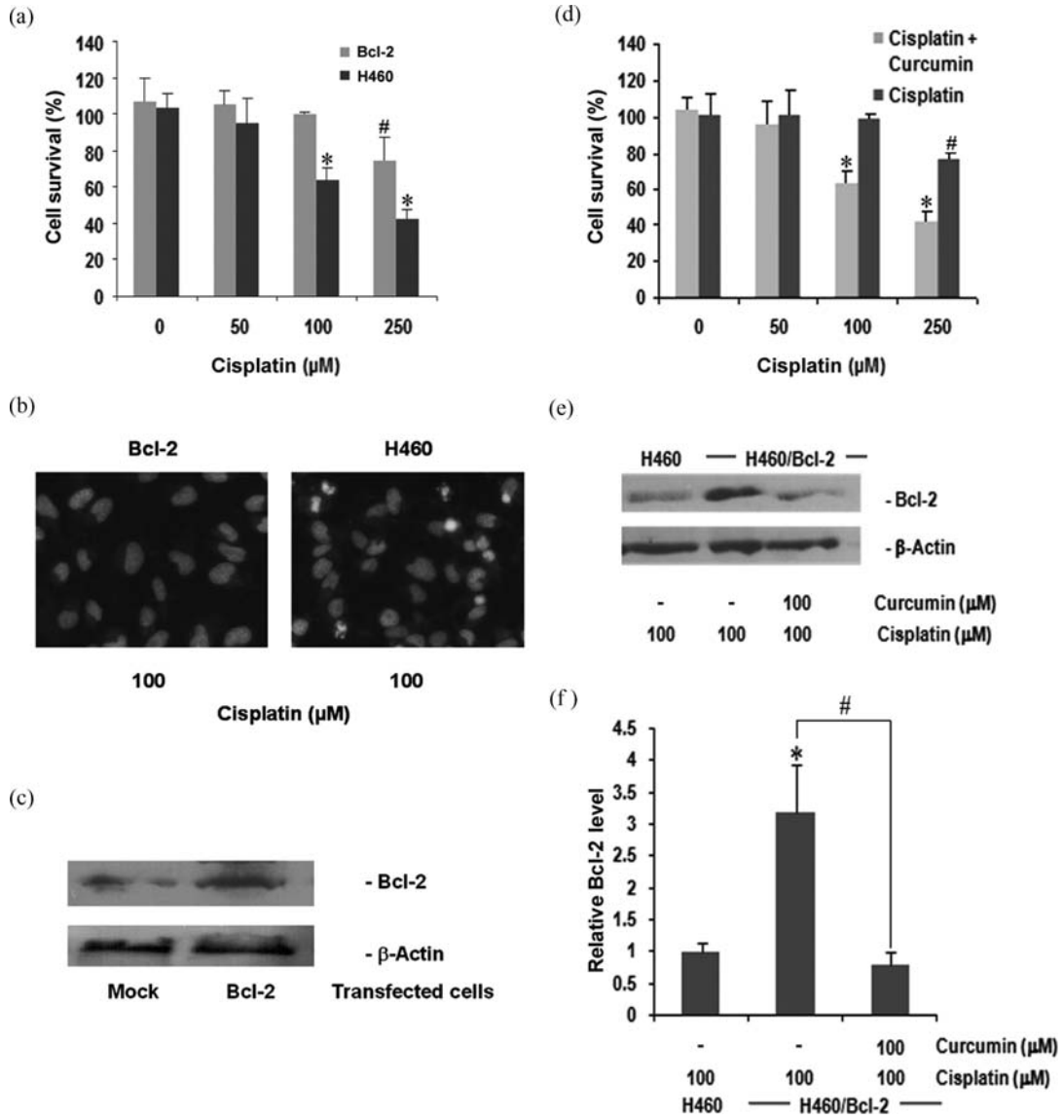

Figure 6. . Bcl-2 mediates cisplatin resistance and its reversal by curcumin. (a) Bcl-2 overexpression increases cisplatin resistance in H460 cells. Cells were transfected with Bcl-2 or control pcDNA3 plasmid as described under Materials and Methods. The transfected cells were exposed to the increasing concentrations of cisplatin (0–250 μmol/L) for 24 hr and cell viability was determined by MTT assay. Values are means $\pm$ SD ($n = 3$). * and #, $p < 0.05$ versus non-treated control. (b) Morphology of apoptotic nuclei of Bcl-2- or control-transfected cells treated with cisplatin (100 μmol/L). (c) Bcl-2 expression levels of Bcl-2- or control-transfected cells determined by Western blot analysis. (d) Curcumin reverses Bcl-2-mediated cisplatin resistance. Bcl-2 overexpressing H460 cells were treated with cisplatin (0–250 μmol/L) or co-treated with cisplatin (0–250 μmol/L) and curcumin (100 μmol/L) for 24 hr. Cell viability was then determined by MTT assay. (e) Curcumin down-regulates Bcl-2 in Bcl-2 overexpressing cells. Control or Bcl-2 overexpressing H460 cells were treated with cisplatin (100 μmol/L) in the presence or absence of curcumin (100 μmol/L) for 24 hr, and analyzed for Bcl-2 expression. Blots were reprobed with β-actin antibody to confirm equal loading of samples. (f) The immune complexes were quantified by densitometry and mean data from independent experiments were normalized to the result obtained in non-treated H460 cells. Values are means $\pm$ SD ($n = 3$). *, $p < 0.05$ versus cisplatin-treated H460 cells; #, $p < 0.05$ versus cisplatin-treated Bcl-2 overexpressing cells.

Inhibition of ROS generation by antioxidant NAC inhibited the down-regulating effect of curcumin on Bcl-2, supporting the above notion. Cisplatin also induced down-regulation of Bcl-2; however, co-administration with curcumin further decreased the Bcl-2 expression and potentiated the apoptotic effect of cisplatin.

The ability of cisplatin and curcumin to induce intracellular ROS generation has been reported in many studies. Co-treatment of the cells with these two pro-oxidants is expected to have a synergistic effect on ROS generation. However, our results show that ROS generation induced by the combined treatment seemed to be caused primarily by curcumin since (1) curcumin

treatment alone induced similar ROS generation as that induced by the combined treatment (Figure 2(b)), and (2) increasing the dose of cisplatin (up to 250 μmol/L) in the combined treatment did not further increase the ROS level (data not shown). It is possible that curcumin induced ROS generation through the same mechanism that was used by cisplatin and that this mechanism had a limited ROS-generating capacity. Mitochondria has been shown to be the primary source of intracellular ROS and curcumin-induced ROS generation was shown to be associated with mitochondrial chain reaction (47, 48). Cisplatin has also been shown to induce ROS generation through mitochondrial respiratory chain reaction by interfering with complex I to IV (49). Together, these studies support our finding and suggest that both cisplatin and curcumin may share the same ROS-inducing mechanism through the mitochondrial pathway.

To further identify the specific ROS involved in this process, we studied the effect of various known inhibitors of ROS on curcumin-induced Bcl-2 down-regulation in cisplatin-treated cells. We found that the superoxide anion scavenger MnTBAP was effective in inhibiting the Bcl-2 down-regulation, whereas the hydrogen peroxide scavenger catalase and the hydroxyl radical scavenger sodium formate were ineffective. Similar effect was observed on cell apoptosis, indicating the essential role of superoxide anion in the apoptosis-sensitizing effect of curcumin through Bcl-2 down-regulation. These results are consistent with a previous report showing that superoxide anion was the dominant ROS induced by curcumin (50).

The mechanism by which superoxide anion mediates the down-regulation of Bcl-2 by curcumin was shown to involve proteasomal degradation of the protein since treatment of the cells with a specific proteasome inhibitor lactacystin or MG132 completely inhibited the down-regulation. Lysosomal degradation plays a minor role in the down-regulation process since lysosome inhibitor CMA had no significant inhibitory effect. This result is consistent with previous reports showing proteasomal degradation of Bcl-2 as a major pathway of its down-regulation by a variety of apoptotic stimuli including ROS (14, 29). Thus, by inducing proteasomal degradation of Bcl-2, curcumin could decrease the anti-apoptotic function of the protein, rendering cells susceptible to apoptosis induction by cisplatin. The importance of Bcl-2 in cisplatin resistance and its reversal by curcumin was demonstrated by the observations that overexpression of Bcl-2 increased cisplatin resistance and curcumin was able to reverse this effect.

In summary, our results reveal a novel mechanism of apoptosis sensitization of curcumin in cisplatin-induced apoptosis of human lung cancer cells. This effect of curcumin is mediated, at least in part, through superoxide anion-dependent down-regulation of Bcl-2 via the proteasomal degradation pathway. Since increased stability and expression of Bcl-2 has been associated with many cancer cell types and is responsible for the inefficacy of many chemotherapeutic agents, the results of this study could have a wide implication in the treatment of cancers. Additional studies verifying the effect of curcumin in other cancer cells and in animal models will be necessary to substantiate the current finding and its potential use as a chemo-sensitizing agent in cancer chemotherapy.

DECLARATION OF INTEREST

The authors report no conflict of interest. The authors alone are responsible for the content and writing of this paper.

ACKNOWLEDGMENTS

Authors are grateful to Dr. Christian Stehlik (Northwestern University, Chicago, IL) for providing Bcl-2 plasmid. This research was supported by The Thailand Research Fund (MRG G5080134 and 5.Q.CU/50/A.1), Drug and Cosmetic Delivery Research Center, and Grant for Development of New Faculty Staff, Chulalongkorn University.

REFERENCES

1. Nishio, K.; Nakamura, T.; Koh, Y.; Suzuki, T.; Fukumoto, H.; Saijo, N. Drug resistance in lung cancer. Curr Opin Oncol **1999**, *11*, 109–115.
2. Wong, E.; Giandomenico, C.M. Current status of platinum-based antitumor drugs. Chem Rev **1999**, *99*, 2451–2466.
3. Seve, P.; Dumontet, C. Chemoresistance in non-small cell lung cancer. Curr Med Chem Anti-Canc Agents **2005**, *5*, 73–88.
4. Roth, B.J.; Bajorin, D.F. Advanced bladder cancer: the need to identify new agents in the post-M-VAC (methotrexate, vinblastine, doxorubicin and cisplatin) world. J Urol **1995**, *153*, 894–900.
5. Hoffman, P.C.; Mauer, A.M.; Vokes, E.E. Lung cancer. Lancet **2000**, *355*, 479–485.
6. Kelly, S.L.; Basu, A.; Teicher, B.A.; Hacker, M.P.; Hamer, D.H.; Lazo, J.S. Overexpression of metallothionein confers resistance to anticancer drugs. Science **1988**, *241*, 1813–1815.
7. Godwin, A.K.; Meister, A.; O'Dwyer, P.J.; Huang, C.S.; Hamilton, T.C.; Anderson, M.E. High resistance to cisplatin in human ovarian cancer cell lines is associated with marked increase of glutathione synthesis. Proc Natl Acad Sci USA **1992**, *1*, 3070–3074.
8. Andrews, P.A.; Schiefer, M.A.; Murphy, M.P.; Howell, S.B. Enhanced potentiation of cisplatin cytotoxicity in human ovarian carcinoma cells by prolonged glutathione depletion. Chem Biol Interact **1988**, *65*, 51–58.
9. Miyake, H.; Hanada, N.; Nakamura, H.; Kagawa, S.; Fugiwara, T.; Hara, I.; Eto, H.; Gohji, K.; Arakawa, S.; Kamidono, S.; Saya, H. Overexpression of Bcl-2 in bladder cancer cells inhibits apoptosis induced by cisplatin and adenoviral-mediated p53 gene transfer. Oncogene **1998**, *19*, 933–943.
10. Li, D.; Ueta, E.; Kimura, T.; Yamamoto, T.; Osaki, T. Reactive oxygen species (ROS) control the expression of Bcl-2 family proteins by regulating their phosphorylation and ubiquitination. Cancer Sci **2004**, *95*, 644–650.
11. Raspollini, M.R.; Castiglione, F.; Degl'Innocenti, D.R.; Baroni, G.; Amunni, G.; Villanucci, A.; Taddei, G.L. Bcl-2 in ovarian carcinoma: a clinicopathologic, immunohistochemical, and molecular study. Pathologica **2004**, *96*, 465–469.
12. Yang, X.; Zheng, F.; Xing, H.; Gao, Q.; Wei, W.; Lu, Y.; Wang, S.; Zhou, J.; Hu, W.; Ma, D. Resistance to chemotherapy-induced apoptosis via decreased caspase-3 activity and overexpression of antiapoptotic proteins in ovarian cancer. Cancer Res Clin Oncol **2004**, *130*, 423–428.
13. Kausch, I.; Jiang, H.; Thode, B.; Doehn, C.; Kruger, S.; Joeham, D. Inhibition of bcl-2 enhances the efficacy of chemotherapy in renal cell carcinoma. Eur Urol **2005**, *47*, 703–709.

14. Chanvorachote, P.; Nimmannit, U.; Stehlik, C.; Wang, L.; Jiang, B.; Ongpipatanakul, B.; Rojanasakul, Y. Nitric oxide regulates cell sensitivity to cisplatin-induced apoptosis through S-nitrosylation and inhibition of Bcl-2 ubiquitination. Cancer Res **2006**, *66*, 6353–6360.
15. Ikegaki, N.; Katsumata, M.; Minna, J. Expression of bcl-2 in small cell lung carcinoma cells. Cancer Res **1994**, *54*, 6–8.
16. Ben-Ezra, J.M.; Kornstein, M.J.; Grimes, M.M. Small cell carcinomas of the lung express the bcl-2 protein. Am J Pathol **1994**, *145*, 1036–1040.
17. Hochstrasser, M. Ubiquitin-dependent protein degradation. Annu Rev Genet **1996**, *30*, 405–439.
18. Ciehanover, A.; Schwartz, A.L. The ubiquitin-proteasome pathway: the complexity and myriad functions of protein deaths. Proc Natl Acad Sci USA **1998**, *95*, 2727–2730.
19. Conney, A.H.; Lysz, T.; Ferraro, T.; Abidi, T.F.; Manchand, P.S.; Laskin, J.D.; Huang, M.T. Inhibitory effect of curcumin and some related dietary compounds on tumor promotion and arachidonic acid metabolism in mouse skin. Adv Enzyme Regul **1991**, *31*, 385–396.
20. Huang, M.T.; Lysz, T.; Ferraro, T.; Abidi, T.F.; Laskin, J.D.; Conney, A.H. Inhibitory effects of curcumin on *in vitro* lipoxygenase and cyclooxygenase activities in mouse epidermis. Cancer Res **1991**, *51*, 813–819.
21. Ruby, A.J.; Kuttan, G.; Babu, K.D.; Rajasekharan, K.N.; Kuttan, R. Anti-tumour and antioxidant activity of natural curcuminoids. Cancer Lett **1995**, *20*, 79–83.
22. Huang, M.T.; Newmark, H.L.; Frenkel, K. Inhibitory effects of curcumin on tumorigenesis in mice. J Cell Biochem Suppl **1997**, *27*, 26–34.
23. Ireson, C.R.; Jones, D.J.; Orr, S.; Coughtrie, M.W.; Boocock, D.J.; Williams, M.L.; Farmer, P.B.; Steward, W.P.; Gescher, A.J. Metabolism of the cancer chemopreventive agent curcumin in human and rat intestine. Cancer Epidemiol Biomarkers Prev **2002**, *11*, 105–111.
24. Aggarwal, B.B.; Kumar, A.; Bharti, A.C. Anticancer potential of curcumin: preclinical and clinical studies. Anticancer Res **2003**, *23*, 363–398.
25. Yoshino, M.; Haneda, M.; Naruse, M.; Htay, H.H.; Tsubouchi, R.; Qiao, S.L.; Li, W.H.; Murakami, K.; Yokochi, T. Prooxidant activity of curcumin: copper-dependent formation of 8-hydroxy-2′-deoxyguanosine in DNA and induction of apoptotic cell death. Toxicol In Vitro **2004**, *18*, 783–789.
26. Atsumi, T.; Fujisawa, S.; Tonosaki, K. Relationship between intracellular ROS production and membrane mobility in curcumin- and tetrahydrocurcumin-treated human gingival fibroblasts and human submandibular gland carcinoma cells. Oral Dis **2005**, *11*, 236–242.
27. Notarbartolo, M.; Poma, P.; Perri, D.; Dusonchet, L.; Cervello, M.; D'Alessandro, N. Antitumor effects of curcumin, alone or in combination with cisplatin or doxorubicin, on human hepatic cancer cells. Analysis of their possible relationship to changes in NF-κB activation levels and in IAP gene expression. Cancer Lett **2005**, *224*, 53–65.
28. Schweyer, S.; Soruri, A.; Heintze, A.; Radzun, H.J.; Fayyazi, A. The role of reactive oxygen species in cisplatin-induced apoptosis in human malignant testicular germ cell lines. Int J Oncol **2004**, *25*, 1671–1676.
29. Wu, Y.J.; Muldoon, L.L.; Neuwelt, E.A. The chemoprotective agent N-acetylcysteine blocks cisplatin-induced apoptosis through caspase signaling pathway. J Pharmacol Exp Ther **2005**, *312*, 424–431.
30. Park, M.S.; Leon, M.D.; Devarajan, P. Cisplatin induces apoptosis in LLC-PK1 cells via activation of mitochondrial pathways. J Am Soc Nephrol **2002**, *13*, 858–865.
31. Henkels, K.M.; Turchi, J.J. Cisplatin-induced apoptosis proceeds by caspase-3-dependent and-independent pathways in cisplatin-resistant and -sensitive human ovarian cancer cell lines. Cancer Res **1999**, *59*, 3077–3083.
32. Melendez-Zaigla, J.; Cruz, E.; Maldonado, V.; Espinoza, A.M. Mitochondrial changes during the apoptotic process of HeLa cells exposed to cisplatin. Biochem Mol Biol Int **1999**, *47*, 765–771.
33. Green, D.R.; Reed, J.C. Mitochondria and apoptosis. Science **1998**, *28*, 1309–1312.
34. Breitschopf, K.; Haendeler, J.; Malchow, P.; Zeiher, A.M.; Dimmeler, S. Posttranslational modification of bcl-2 facilitates its proteasome-dependent degradation: molecular characterization of the involved signaling pathway. Mol Cell Biol **2000**, *20*, 1886–1896.
35. Sharma, H.; Sen, S.; Singh, N. Molecular pathways in the chemosensitization of cisplatin by quercetin in human head and neck cancer. Cancer Biol Ther **2005**, *4*, 949–955.
36. Muroi, M.; Takasu, A.; Yamasaki, M; Takatsuki, A. Folimycin (concanamycin A), an inhibitor of V-type H (+)-ATPase, blocks cell-surface expression of virus-envelope glycoproteins. Biochem Biophys Res Commun **1993**, *193*, 999–1005.
37. Jung, E.M.; Lim, J.H.; Lee, T.J.; Park, J.W.; Choi, K.S.; Kwon, T.K. Curcumin sensitizes tumor necrosis factor-related apoptosis-inducing ligand (TRAIL)-induced apoptosis through reactive oxygen species-mediated upregulation of death receptor 5 (DR5). Carcinogenesis **2005**, *26*, 1905–1913.
38. Deeb, D.; Jiang, H.; Gao, X.; Hafner, M.S.; Wong, H.; Divine, G.; Chapman, R.A.; Dulchavsky, S.A.; Gautam, S.C. Curcumin sensitizes prostate cancer cells to tumor necrosis factor-related apoptosis-inducing ligand/Apo2L by inhibiting nuclear factor-kappaB through suppression of IkappBalpha phosphorylation. Mol Cancer Ther **2005**, *3*, 803–812.
39. Weir, N.M.; Selvendiran, K.; Kutala, V.K.; Tong, L.; Vishwanath, S.; Rajaram, M.; Vishwanath, S.; Rajaram, M.; Tridandapani, S.; Anant, S.; Kuppusamy, P. Curcumin induces G2/M arrest and apoptosis in cisplatin-resistant human ovarian cancer cells by modulating Akt and p38 MAPK. Cancer Biol Ther **2007**, *6*, 178–184.
40. Singh, S.; Aggarwal, B.B. Activation of transcription factor NF-kappa B is suppressed by curcumin (diferuloylmethane). J Biol Chem **1995**, *270*, 24995–25000.
41. Aggarwal, S.; Ichikawa, H.; Takada, Y.; Sandur, S.K.; Shishodia, S.; Aggrawal, B.B. Curcumin (diferuloylmethane) down-regulates expression of cell proliferation, antiapoptotic, and metastatic gene products through suppression of IκBα kinase and AKT activation. Mol Pharmacol **2006**, *69*, 195–206.
42. Woo, J.H.; Kim, Y.H.; Choi, Y.J.; Kim, D.G.; Lee, K.S.; Bae, J.H.; Min, D.S.; Chang, J.S.; Jeong, Y.J.; Lee, Y.H.; Park, J.W.; Kwon, T.K. Molecular mechanisms of curcumin-induced cytotoxicity: induction of apoptosis through generation of reactive oxygen species, down-regulation of Bcl-XL and IAP, the release of cytochrome c and inhibition of Akt. Carcinogenesis **2003**, *24*, 1199–1208.
43. Siddick, Z.H. Cisplatin: mode of action and molecular basis of resistance. Oncogene **2003**, *22*, 7265–7279.
44. Adams, J.M.; Cory, S. Life-or-death decisions by the Bcl-2 protein family. Trends Biochem Sci **2001**, *26*, 61–66.
45. Ohsaki, Y.; Toyoshima, E.; Fujiuchi, S.; Matsui, H.; Hirata, S.; Miyokawa, N.; Kubo, Y.; Kikuchi, K. Bcl-2 and p53 protein expression in non-small cell lung cancers: correlation with survival time. Clin Cancer Res **1996**, *2*, 915–920.
46. Ohmori, T.; Podack, E.R.; Nishio, K.; Takahashi, M.; Miyahara, Y.; Takeda, Y.; Kubota, N.; Funayama, Y.; Ogasawara, H.; Ohira, T.; Ohta, S.; Saijo, N. Apoptosis of lung cancer cells caused by some anti-cancer agents (MMC, CPT-11, ADM) is inhibited by bcl-2. Biochem Biophys Res Commun **1993**, *192*, 30–36.
47. Numsen, H. Mitochondrial reactive oxygen species affect sensitivity to curcumin-induced apoptosis. Free Radic Biol Med **2008**, *44*, 1382–1393.

48. Lenaz G. Role of mitochondria in oxidative stress and ageing. Biochem Biophys Acta **1998**, *1366*, 53–67.
49. Kruidering, M.; Water, B.V.D.; Heer, E.D.; Mulder, G.J.; Nagelkerke, J.F. Cisplatin-induced nephrotoxicity in porcine proximal tubular cells: mitochondrial dysfunction by inhibition of complexes I to IV of the respiratory chain. J Pharmacol Exp Ther **1997**, *280*, 638–649.
50. Bhaumik, S.; Anjum, R.; Rangaraj, N.; Pardhasaradhi, B.V.V.; Khar, A. Curcumin-mediated apoptosis in AK-5 tumor cells involves the production of reactive oxygen intermediates. FEBS Lett **1999**, *456*, 311–314.

Nitric Oxide Regulates Lung Carcinoma Cell Anoikis through Inhibition of Ubiquitin-Proteasomal Degradation of Caveolin-1*

Pithi Chanvorachote†‡, Ubonthip Nimmannit§, Bing-Hua Jiang||, Yon Rojanasakul‡||
†Department of Physiology and §Pharmaceutical Technology (International) Program, Chulalongkorn University, Bangkok 10330, Thailand
||Mary Babb Randolph Cancer Center and ‡Department of Pharmaceutical Sciences, West Virginia University, Morgantown, WV 26506, USA
Running Title: NO Regulates Caveolin-1 and Anoikis
*This work was supported by NIH Grant R01-HL076340
Correspondence: Yon Rojanasakul, West Virginia University, Health Sciences Center, Morgantown, WV 26506, (yrojan@hsc.wvu.edu); Pithi Chanvorachote, Chulalongkorn University, Bangkok 10330, Thailand (pithi_chan@yahoo.com)

Anoikis, a detachment-induced apoptosis, is a principal mechanism of inhibition of tumor cell metastasis. Tumor cell acquiring anoikis resistance, as frequently observed in human lung cancer, becomes an important obstacle of efficient cancer therapy. Recently, signaling mediators such as caveolin-1 (Cav-1) and nitric oxide (NO) have garnered attention in metastasis research; however, their role and the underlying mechanisms of metastasis regulation are largely unknown. Here, we show that NO impairs the apoptotic function of human lung carcinoma H460 cells after detachment. The NO donors sodium nitro prusside and diethylenetriamine NONOate inhibit detachment-induced apoptosis, whereas the NO inhibitors aminoguanidine and 2-(4-carboxyphenyl) tetramethylimidazoline-1-oxyl -3-oxide promote this effect. Resistance to anoikis in H460 cells is mediated by Cav-1, which is significantly downregulated after cell detachment through a non-transcriptional mechanism involving ubiquitin-proteasomal degradation. NO inhibits this downregulation by interfering with Cav-1 ubiquitination through a process that involves protein *S*-nitrosylation, which prevents its proteasomal degradation and induction of anoikis by cell detachment. These findings indicate a novel pathway for NO regulation of Cav-1, which could be a key mechanism of anoikis resistance in tumor cells.

Key words: nitric oxide, anoikis, apoptosis, caveolin-1, ubiquitination

INTRODUCTION

Caveolin-1 (Cav-1), a 21-24 kDa structural protein component of the plasma membrane microdomains termed caveolae has been shown to function in vesicular trafficking, signal transduction, and cancer progression (1-4). While upregulation of this protein is normally occurred in a variety of terminally differentiated cells including fibroblasts, adipocytes, smooth muscle cells, endothelial cells, and epithelial cells (5), Cav-1 is greatly reduced in most oncogenically transformed and cancer cells (6-10). Thus, Cav-1 was first explained to function as a tumor suppressor protein (11-13). In contrast, increasing evidence indicates its role as a tumor and metastatic promoter since over-expression or re-expression of Cav-1 was found in many advanced stage and metastatic cancer cells. Upregulation of Cav-1 was shown to render Rat1A cell more resistant to apoptosis (14) and antisense-induced downregulation of Cav-1 caused human prostate cancer cells more sensitive to apoptosis (15, 16). Therefore, the role of Cav-1 in cancer progression remains controversial.

Metastasis is a multistep process composed of cancer cell detachment, migration and adhesion of the detached cells to other target sites, and extravasation and formation of metastases. A key mechanism in the regulation of metastasis is anoikis or detachment-induced apoptosis. Previous studies have shown that Cav-1 acts as a negative regulator of anoikis (17, 18) and its elevated expression in lung carcinoma is closely associated with the increased metastasis capacity and poor survival of the patients (19). Likewise, elevated NO and NO synthase (NOS) levels have been associated in many human metastatic cancers including the lung (20-24), breast (25), central nervous system (26), and colon (27). However, the role of NO and its mechanism of metastasis regulation in association with Cav-1 are not well understood. Since resistance to anoikis is a key step in metastasis development and since Cav-1 has been implicated in this process, we investigated the potential regulation of Cav-1 by NO and studied its role in anoikis of human lung carcinoma cells.

NO has been reported to have both pro- and anti-apoptotic effect on cells, depending on a variety of factors, including cell type, cellular redox status, and the flux and dose of NO (28, 29). In human lung carcinoma cells, we previously reported that NO plays a suppressive role in apoptosis induced by a variety of agents, including Fas death ligand (30), chemotherapeutic agent cisplatin (31), and metal carcinogen (32). However, the role of NO in cell anoikis and its potential regulation of Cav-1 have not been well investigated. Using molecular and pharmaco logical approaches, we reported here that NO plays an important role in Cav-1 regulation and anoikis function of human lung cancer H460 cells. We also demonstrated for the first time that Cav-1 is downregulated during cell anoikis through the ubiquitin-proteasomal degradation pathway and that NO regulates this process by inducing *S*-nitrosylation of the protein which inhibits its ubiquitination and proteasomal degradation. Thus, our study reveals the existence of a novel mechanism of anoikis regulation, which might be exploited in metastasis and cancer therapy.

MATERIALS and METHODS

Cells and Reagents

Human lung epithelial NCI-H460 cells were obtained from the American Type Culture Collection (Manassas, VA). The cells were cultured in RPMI-1640 medium supplemented with 5% fetal bovine serum (FBS), 2 mM L-glutamine, and 100 units/mL penicillin and streptomycin. Cell cultures were maintained in a humidified atmosphere of 5% CO_2 at 37°C. Cells were passaged at preconfluent densities using a solution containing 0.05% trypsin and 0.5 mM EDTA. Sodium nitro prusside (SNP), 2-(4-carboxyphenyl)-4,4,5,5 tetramethylimidazoline-1-oxy-3-oxide (PTIO), aminoguanidine (AG), dithiothreitol (DTT), annexin V-fluorescein isothiocyanate (FITC), propidium iodide (PI), and lactacystin (LAC) were obtained from Sigma Chemical, Inc. (St. Louis, MO). Diaminofluorescein diacetate (DAF-DA) and Hoechst 33342 were obtained from Molecular Probes, Inc. (Eugene, OR). Monoclonal antibody against Cav-1 and protein A-agarose were from Santa Cruz Biotechnology (Santa Cruz, CA). Antibodies for ubiquitin, *S*-nitrosocysteine, β-actin, and isotype-matched peroxidase-labeled secondary antibodies were from Sigma Chemical Inc. The transfecting agent Lipofectamine 2000 was from Invitrogen (Carlsbad, CA).

NO Detection

Cellular NO production was determined by flow cytometry using DAF-DA as a fluorescent probe and by Griess assay which measures the stable nitrite byproduct of NO in the culture medium. After detachment, cells ($1x10^6$/mL) were collected and incubated with

10 μM DAF-DA for 30 min at 37°C. The cells were then washed, resuspended in phosphate-buffered saline (PBS), and analyzed for fluorescence intensity using FACSCaliber (Becton-Dickinson, Rutherford, NJ). Signals were obtained using a 488-nm excitation beam and a 538-nm band-pass filter. In some experiments, cells were visualized for fluorescence intensity using a fluorescence microscope (Carl Zeiss Axiovert, Göttingen, Germany). For Griess assay, cell supernatants were collected and aliquots (100 μL) were mixed with 100 μL Griess reagent (1% sulfanilamide/0.1% naphthylethylene diamine dihydrochloride/2% phosphoric acid) in a 96-well plate. After incubation for 10 min at 25°C, the absorbance at 550 nm was measured on a microplate reader.

Plasmid and Transfection

Caveolin-1 plasmid (pEX_Cav-1-YFP) was obtained from the American Type Culture Collection (Manassas, VA). Stable transfectant of Cav-1 was generated by culturing H460 cells in a six-well plate until they reached 60% confluence. One microgram of cytomegalovirus-neo vector and 15 μL of Lipofectamine reagent with 2 μg of Cav-1 or control pcDNA3 plasmid were used to transfect the cells in the absence of serum. After 12 h, the medium was replaced with culture medium containing 5% FBS. Approximately 36 h after the beginning of the transfection, the cells were digested with 0.03% trypsin, and the cell suspensions were plated onto 75-mL culture flasks and cultured for 24 to 28 d with G418 selection (600 μg/mL). The pooled stable transfectant was identified by Western blot analysis of Cav-1 and was cultured in G418-free RPMI-1640 medium for at least two passages before each experiment.

Anoikis Assays

Adherent H460 cells in culture were trypsinized into a single cell suspension and then seeded in 12-well tissue culture plates coated with 200 μL (6 mg/mL in 95% ethanol) of poly-(2-hydroxyethyl methacrylate) (poly-HEME; Sigma Chemical Inc.) at the density of $1x10^5$ cells/mL. Suspended cells were incubated at 37°C for various times up to 24 h. Cells were then harvested, washed, and stained with annexin V-FITC and analyzed for fluorescence intensity by flow cytometry and fluorescence microscopy. For Hoechst 33342 apoptosis assay, cells were incubated with 10 μM of the Hoechst dye for 30 min at 37°C, and the apoptotic cells having intensely condensed chromatin and/or fragmented nuclei were visualized under a fluorescence microscope. For cell survival assay, cells were similarly treated, harvested, washed, and incubated with 20 μM of sodium 2,3-bis(2-methoxy-4-nitro-5-sulfophenyl)-2H-tetrazolium-5-carboxanilide (XTT) for 4 h at 37ºC. Optical density was then determined by V-max photometer (Molecular Devices, Inc., Menlo Park, CA) at a wavelength of 450 nm.

Western Blot Analysis

Cell extracts were performed by incubating the cells in lysis buffer containing 20 mM Tris-HCl, pH 7.5, 1% Triton X-100, 150 mM sodium chloride, 10% glycerol, 1 mM sodium orthovanadate, 50 mM sodium fluoride, 100 mM phenylmethylsulfonyl fluoride, and a protease inhibitor mixture (Roche Molecular Biochemicals, Basel, Switzerland) for 30 min on ice. Cell lysates were collected and assayed for protein content using the Bradford method (Bio-Rad Laboratories, Hercules, CA). Equal amount of proteins per sample (40 μg) were resolved on a 10% SDS-polyacrylamide gel electrophoresis and transferred onto 0.45-μm nitrocellulose membranes (Pierce, Rockford, IL). The transferred membranes were blocked for 1 h in 5% nonfat dry milk in Tris-buffered saline/Tween 20 (25 mM Tris-HCl, pH 7.4, 125 mM NaCl, and 0.05% Tween 20) and incubated with appropriate primary antibodies at 4°C overnight. Membranes were washed

three times with Tris-buffered saline/Tween 20 for 10 min and incubated with peroxidase-labeled secondary antibodies for 1 h at room temperature. The immune complexes were detected by chemiluminescence (Supersignal West Pico; Pierce) and quantified by imaging densitometry using analyst/PC densitometry software (Bio-Rad, Richmond, CA).

Immunoprecipitation

Cells were washed after treatments and lysed in lysis buffer for 30 min on ice. Cell lysates were collected and determined for protein content. Equal amount of proteins per sample (60 μg) were immunoprecipitated with anti-Cav-1 antibody for 6 h at 4°C. The immune complexes were washed with 30 volumes of lysis buffer, resuspended in 2X Laemmli sample buffer, and boiled at 95°C for 5 min. The immune complexes were separated by 10% SDS-PAGE and analyzed by Western blotting as described above.

Measurements of Cav-1 S-nitrosylation

Cells were lysed and immunoprecipitated with anti-Cav-1 antibody as described above. The immunoprecipitated protein was analyzed for *S*-nitrosylation by Western blot using anti-*S*-nitrosocysteine antibody and by fluorometric measurements as previously described (32). Briefly, immunoprecipitates were incubated with 200 μM $HgCl_2$ and 200 μM diamino naphthalene (DAN) in 500 μL PBS for 0.5 h at room temperature followed by the addition of 1 M NaOH. The fluorescent triazole product generated from the reaction between DAN and NO released from *S*-nitrosylated Cav-1 was quantified by fluorometry at the excitation and emission wavelengths of 375 and 450 nm, respectively.

Reverse transcription-PCR

Total RNA was extracted with TRIZOL (Invitrogen, Carlsbad, CA) and reverse transcription-PCR was performed with Access RT-PCR System (Promega, Madison, WI), according to the manufacturer's instructions. Sequences of the PCR primers for Cav-1 were forward, 5'-CGTAGACTCGGAGGGACATC-3'; reverse, 5'-TTTCGTCACAGTGAAGGTGG-3'; glyceraldehyde-3-phosphate dehydrogenase (GAPDH) were forward, 5'-GCTGAGAACGGGAAGCTTGT-3'; reverse, 5'-GCCAGGGGTGCTAAGCAG-3'. Reaction products were analyzed after 30 amplification cycles, each of which involved consecutive 1-min steps at 94°C, 55°C and 72°C. The PCR products were electrophoresed in a 1.5% agarose gel, stained with ethidium bromide, and photographed.

Statistical Analysis

Data were represented as means ± SD from three or more independent experiments. Statistical analysis was performed by Student's *t* test at a significance level of $p < 0.05$.

RESULTS

Nitric Oxide Inhibits Detachment-Induced Apoptosis of H460 Cells

NO has been shown to play an important role in the regulation of cancer cell metastasis; however, the underlying mechanism of this regulation is unclear. To test whether NO might regulate this process by inhibiting detachment-induced apoptosis or anoikis which is a crucial step in the metastasis of cancer cells, we first investigated anoikis of human lung cancer H460 cells in response to various specific NO donors and inhibitors. Anoikis was induced by detaching the cells and incubating them in attachment-resistant poly-HEME-coated plates for various times and analyzed for cell viability by XTT assay. Figure 1*A* shows that detachment of the cells caused a time-dependent decrease in cell viability with approximately 55% and 15% of the cells remained viable after 6 and 12 h, respectively. Analysis of cell apoptosis by flow cytometry using FITC-labeled annexin V

antibody shows a significant increase in annexin V-associated cellular fluorescence as early as 6 h after the detachment and reached a maximum at about 18 h (Fig. 1*B*). In contrast, analysis of cell necrosis using propidium iodide (PI) as a probe shows no significant increase in the PI signal over a 24-h period. These results suggest that apoptosis is the primary mode of cell death after detachment of H460 cells. Morphologic analysis of apoptotic cell death by fluorescence microscopy using Hoechst 33342 and annexin V-FITC further confirms the results (Fig. 1*E*).

To investigate the role of NO in detachment-induced apoptosis, detached H460 cells were treated with various concentrations of NO donors and inhibitors, and their effect on cell survival was determined by XTT assay. Figure 1*C* shows that treatment of the cells with NO donor, sodium nitroprusside (SNP) or dipropylenetriamine (DETA) NONOate, caused a dose-dependent decrease in cell death, whereas treatment of the cells with NO inhibitor, aminoguanidine (AG) or 2-(4-carboxyphenyl) tetramethylimidazoline-1-oxy -3-oxide (PTIO), had an opposite effect. Analysis of cell apoptosis by annexin V-FITC and Hoechst 33342 assays similarly shows the inhibitory and promoting effect of the NO donors and inhibitors respectively on detachment-induced cell death (Fig. 1, *D* and *E*). The NO donors and inhibitors, when used at the indicated concentrations, had no significant effect on cell necrosis as determined by PI assay (Fig. 1*D*).

Effect of NO Modulators on Cellular NO Level

To provide a relationship between cell death and NO modulation induced by the test agents, we analyzed cellular NO levels in response to various NO modulator treatments by colorimetric Griess assay and by flow cytometric and microscopic assays using DAF-DA as a fluorescent probe for NO. Figure 2*A* shows the result of the Griess assay which measures the stable nitrite breakdown product of NO. Both NO inhibitors AG and PTIO significantly inhibited cellular nitrite production, whereas the NO donors SNP and DETA NONOate increased the production, as compared to non-treated control. These results were confirmed by flow cytometric and microscopic assays of NO (Fig. 2, *B* and *C*), which show the induction and inhibition of cellular NO levels by the NO donor SNP and NO inhibitor PTIO, respectively.

Cav-1 Overexpression Renders H460 Cells Resistant to Detachment-Induced Apoptosis

The role of Cav-1 in the regulation of cancer cell anoikis is unclear. We studied this role by stably transfecting H460 cells with Cav-1 or control plasmid, and evaluated their effect on detachment-induced cell death. Transfected cells were detached, suspended in poly-HEME-coated plates, and analyzed for cell survival at various times by XTT assay. Figure 3*A* shows that Cav-1-transfected cells exhibited resistance to detachment-induced cell death as compared to control-transfected cells. Western blot analysis of Cav-1 expression in the transfected cells shows an increased expression of Cav-1 protein in the Cav-1-transfected cells as compared to control-transfected cells (Fig. 3*B*). These results indicate the role of Cav-1 as a positive regulator of cell anoikis in lung epithelial H460 cells.

Cav-1 Overexpression Alters Cell Growth and Morphology of H460 Cells

Figure 3*C* shows that under a normal growth condition that allows cell attachment, Cav-1 overexpressing cells exhibited an increased growth rate over control-transfected cells. The lag phase prior to cell growth was significantly reduced in Cav-1 overexpressing cells. As compared to control-transfected cells which grew as an epithelial monolayer, Cav-1 overexpressing cells formed cell

mounds and grew as multilayer epithelial cells (Fig. 3*D*). This multilayer growth pattern is consistent with the increased growth rate of Cav-1 overexpressing cells. These results suggest that Cav-1 may function as a tumor promoter by enhancing cell growth and oncogenic transformation.

Detachment Induces Cav-1 Downregulation through a Non-Transcriptional Proteasome-Dependent Mechanism

Having demonstrated the role of Cav-1 as a negative regulator of cell anoikis in H460 cells, we next investigated the expression profile of Cav-1 after cell detachment. Detached cells were suspended in attachment-resistant plates for various times and analyzed for Cav-1 protein and mRNA expression by Western blotting and RT-PCR, respectively. Figure 4*A* shows that Cav-1 protein levels were significantly reduced in cells after detachment in a time-dependent manner. The reduction was strongly inhibited by lactacystin (LAC), a specific proteasome inhibitor, suggesting that detachment-induced Cav-1 downregulation was mediated through proteasomal degradation. This result was confirmed by the observation that another proteasome inhibitor, MG132, also inhibited the decrease in Cav-1 protein expression (data not shown). Analysis of Cav-1 mRNA levels show that Cav-1 transcripts were relatively unchanged after cell detachment (Fig. 4*B*), while the protein levels were substantially reduced. Thus, cell detachment appears to cause Cav-1 protein reduction through a transcription-independent mechanism. These results along with subsequent data showing the effect of cell detachment on Cav-1 ubiquitination support the role of ubiquitin-proteasomal degradation as an important mechanism of Cav-1 downregulation induced by cell detachment.

Nitric Oxide Prevents Detachment-Induced Cav-1 Downregulation

We further investigated the potential regulation of Cav-1 by NO. Cells were detached and suspended in HEMA-coated plates in the presence or absence of NO donors and inhibitors. Cav-1 protein expression was then determined by Western blotting. Figure 4*C* shows that the NO donors SNP and DETA NONOate strongly inhibited detachment-induced Cav-1 downregulation at the concentrations shown to induce an increase in cellular NO levels (Fig. 2). In contrast, the NO inhibitors AG and PTIO promoted this downregulation (Fig. 4*C*), supporting the suppressive role of NO in detachment-induced Cav-1 downregulation.

Detachment Induces Cav-1 Ubiquitination and Its Inhibition by NO

The observation that detachment-induced Cav-1 downregulation was inhibited by proteasome inhibitors suggest that this downregulation could be mediated by protein ubiquitination and subsequent degradation by the proteasome. Since ubiquitination of Cav-1 has not been reported, we examined whether cell detachment could induce Cav-1 ubiquitination and whether or not this process is regulated by NO. Cells were detached and suspended in HEMA-coated plates in the presence or absence of NO donors for various times. Cell lysates were prepared, immuno-precipitated with anti-Cav-1 antibody, and the resulting immune complexes were analyzed for ubiquitin by Western blotting. Figure 5*A* shows that Cav-1 was rapidly ubiquitinated as early as 1 h after cell detachment and peaked at about 3 h. The NO donors SNP and DETA NONOate strongly inhibited this ubiquitination, suggesting that NO-mediated inhibition of protein ubiquitination could be a key mechanism of Cav-1 stabilization by NO and our subsequent study supports this notion.

NO-Mediated S-Nitrosylation of Cav-1 as a Potential Mechanism of Protein Stability Regulation

Previous studies have shown that NO induced *S*-nitrosylation of some apoptosis-regulatory proteins, such as c-FLIP and Bcl-2, and prevented their ubiquitination and degradation by the proteasome (30-32). To test whether *S*-nitrosylation could be involved in the regulation of Cav-1 by NO, we performed immunoprecipitation experiments examining the effect of NO on Cav-1 *S*-nitrosylation and protein expression. The results show that treatment of the cells with NO donors, SNP and DETA NONOate, induced *S*-nitrosylation of Cav-1 as determined by Western blot analysis of the immunoprecipitated protein using *S*-nitrosocysteine antibody (Fig. 5*B*). Similar results were obtained when the immunoprecipitated protein was analyzed for *S*-nitrosylation by fluorometric measurements of the released NO product (Fig. 5*C*). Cav-1 *S*-nitrosylation by the NO donors was inhibited by DTT, a known inhibitor of *S*-nitrosylation (33, 34) (Fig. 5, *B* and *C*), supporting the specificity of *S*-nitrosylation detection. To test whether *S*-nitrosylation of Cav-1 affects its stability, we analyzed the effect of NO donors and DTT on Cav-1 protein expression. Figure 6*A* shows that the NO donors SNP and DETA NONOate were able to stabilize the protein after cell detachment and that the *S*-nitrosylation inhibitor DTT inhibited the stabilizing effect of NO donors. Together, these results indicate that NO regulates Cav-1 expression, at least in part, by inducing protein *S*-nitrosylation which interferes with its ubiquitination and subsequent degradation by the proteasome. This new finding provides a mechanistic insight into the regulation of Cav-1 by NO, which could be important in the control of cancer cell anoikis and metastasis.

Nitric Oxide Induces Anoikis Resistance and Multilayer Formation

To provide supporting evidence for the role of NO in the regulation of cell anoikis through protein *S*-nitrosylation, H460 cells were detached and incubated with NO donors in the presence or absence of DTT. Cell viability was then determined after 12 h using XTT assay. Figure 6*B* shows that the NO donors SNP and DETA NONOate significantly increased cell viability after detachment and that DTT inhibited this effect of NO donors. In the earlier study, we showed that cells over-expressing Cav-1 exhibited multilayer formation. Since NO upregulates Cav-1 expression, we examined whether NO could induce a similar multilayer formation in H460 cells. Cells were grown in culture plates in the presence or absence of NO donors and cell morphology was examined by microscopy after 24 h. Figure 6*B* shows that the NO donors SNP and DETA NONOate were able to induce multilayer formation of H460 cells as compared to non-treated control. Since multilayer formation is a key characteristic of malignant tumor cells, this finding suggests that NO may regulate tumorigenesis by promoting malignant transformation through Cav-1 upregulation.

DISCUSSION

Lung cancer is the leading cause of cancer mortality worldwide and most of the death is associated with tumor metastasis. To metastasize, a malignant cell must detach from its primary tumor, invade the nearby circulatory or lymph system, and establish itself in a new site. Once in the bloodstream, most of the cells die by anoikis which is an important mechanism that prevents metastasis. However, some cancer cells develop resistance to anoikis and consequently survive to establish new metastases. Several anoikis-regulatory proteins including Cav-1 have been investigated in recent years. However, the role of Cav-1 in metastatic cancer progression and the underlying mechanisms are unclear. Both pro- and anti-carcinogenic effect of Cav-1 have been described. Recombinant Cav-1 overexpression was shown to inhibit cell

proliferation by inducing cell cycle arrest at G_0/G_1 phase (1). Genomic analysis of Cav-1(-/-) null mice and human breast cancer mutations (P132L) supported the role of Cav-1 as a negative regulator of cell transformation and tumorigenesis (35). Likewise, stable expression of Cav-1 in human breast cancer MCF-7 cells attenuated cell proliferation and inhibited anchorage-independent growth (17). In contrast to its suppressive role in cancer cell growth, an elevated expression of Cav-1 has been reported in several human tumors including prostate, colon, and breast (23, 24). Overexpression of Cav-1 also prevented detachment-induced apoptosis and p53 activation in cancer cells (18). Furthermore, in lung cancer cells Cav-1 overexpression promoted metastasis (19). Consistent with the pro-survival role of Cav-1, we found that Cav-1 positively regulated cell growth and inhibited anoikis of lung cancer H460 cells. Cav-1 was rapidly downregulated after cell detachment (Fig. 4) and overexpression of Cav-1 or stabilization of the protein by NO protected the cells from apoptosis (Figs. 3 and 6). NO induction and Cav-1 overexpression also promoted cell transformation facilitating multilayer formation (Figs. 3 and 6).

The expression of Cav-1 is tightly regulated at various levels, including transcriptional and post-transcriptional (for review, see Ref. 36). Although the importance of transcriptional regulation of Cav-1 has been emphasized in numerous studies, post-translational modifications such as ubiquitination and phosphorylation have emerged as important regulators of protein stability and function (for reviews, see Ref. 29, 37). In the present study, we found that Cav-1 was rapidly ubiquitinated and degraded by the proteasome after cell detachment in concomitant with anoikis (Figs. 4 and 5). Cav-1 transcripts were relatively unchanged during this process (Fig. 4), indicating a non-transcriptional control of Cav-1 expression after cell detachment. These results support the ubiquitin-proteasomal degradation as a primary mechanism of detachment-induced Cav-1 downregulation. This finding adds Cav-1 to the growing list of cellular proteins that are subjected to regulation by the ubiquitin-proteasomal degradation pathway.

The results of this study also demonstrated that Cav-1 stability and function is regulated by NO. NO has been shown to regulate apoptosis under various physiologic and pathologic conditions (28, 38, 39); however, its role in anoikis and its regulation of Cav-1 have not been well investigated. We showed that NO negatively regulates anoikis of lung epithelial H460 cells as demonstrated by the ability of NO donors to suppress detachment-induced apoptosis and the reversal effect induced by NO inhibitors (Fig. 1). The NO donors also had a stabilizing effect on detachment-induced Cav-1 downregulation, whereas the NO inhibitors showed an opposite effect (Fig. 6). These results support NO-mediated stabilization of Cav-1 as a key mechanism of anoikis regulation. The mechanism by which NO stabilizes Cav-1 was shown to involve inhibition of protein ubiquitination since the NO donors inhibited the ubiquitination of Cav-1 by cell detachment (Fig. 5).

Recent evidence indicate that *S*-nitrosylation is an important mechanism by which NO modulates the function of cellular proteins (for reviews, see Ref. 29, 40). *S*-nitrosylation can either attenuate or accentuate protein functions (41-43) and our previous studies have shown that it plays an important role in stability and function of apoptosis-regulatory proteins such as c-FLIP and Bcl-2 (30-32). In the present study, we found that Cav-1 was rapidly *S*-nitrosylated by NO after cell detachment and inhibition of this *S*-nitrosylation by DTT blocked the effect of NO on Cav-1 ubiquitination (Fig. 5), suggesting the

regulation of ubiquitination by *S*-nitrosylation. The inhibition of *S*-nitrosylation by DTT also led to a decrease in Cav-1 protein expression and cell survival (Fig. 6), supporting the role of *S*-nitrosylation in Cav-1 stability and function. The mechanism by which *S*-nitrosylation promotes Cav-1 stability was shown to involve protein ubiquitination inhibition, although the precise mechanism of this inhibition remains to be investigated. It is possible that *S*-nitrosylation of Cav-1 may alter the protein conformation such that it could not be recognized by the enzyme ubiquitin ligases that serve to tag the protein for subsequent degradation by the proteasome.

In conclusion, we demonstrated that Cav-1 plays an important role as a negative regulator of anoikis in human lung carcinoma H460 cells. We also demonstrated for the first time that Cav-1 is downregulated during cell anoikis through a non-transcriptional mechanism involving ubiquitin-proteasomal degradation, and that NO regulates this process, at least in part, through protein *S*-nitrosylation which prevents its ubiquitination and degradation by the proteasome. In demonstrating the effect of NO on Cav-1 stability and function, we documented a novel mechanism of anoikis regulation, which could be important in the control of cancer metastasis. Because NO and Cav-1 have been shown to be overexpressed in many human tumors, NO-mediated regulation of Cav-1 could be a common mechanism of anoikis resistance and metastasis of other cancers. This novel finding on the regulation of Cav-1 by NO may have important implications in cancer therapy.

FOOTNOTES

This work was supported by the National Institutes of Health (R01-HL076340) and Thailand Research Fund and Commission on Higher Education (MRG G5080134).

The abbreviations used are: NO, nitric oxide; Cav-1, caveolin-1; SNP, sodium nitroprusside; DPTA, dipropylenetriamine; AG, aminoguanidine; PTIO, 2-(4-carboxyphenyl)-4,4,5,5-tetra methyl-imidazoline-1-oxyl-3-oxide; LAC, lactacystin; DTT, dithiothreitol; DAF-DA, diamino-fluorescein diacetate

REFERENCES

1. Galbiati, F., Volonte, D., Liu, J., Capozza, F., Frank, P.G., Zhu, L., Pestell, R.G., and Lisanti, M.P. (2001) *Mol. Biol. Cell* **12**, 2229-2244
2. Glenney, J.R. and Zokas, L. (1989) *J. Cell. Biol*. **108**, 2401-2408
3. Rothberg, K., Heuser, J.E., Donzell, W.C., Ying, Y.S., Glenney, J.R., and Anderson, R.G.W. (1992) *Cell* **68**, 673-682
4. Scherer, P.E., Okamoto. T., Chun, M., Nishimoto, I., Lodish, H.F., and Lisanti, M.P. (1996) *Proc. Natl. Acad. Sci. USA* **93**, 131-135
5. Razani, B., Schlegel, A., Liu, J., and Lisanti, M.P. (2001) *Biochem. Soc. Trans.* **29**, 494-499
6. Koleske, A.J., Baltimore, D., and Lisanti, M.P. (1995) *Proc. Natl. Acad. Sci. USA* **92**, 1381-1385
7. Engelman, J.A., Chu, C., Lin, A., Jo, H., Ikezu, T., Okamoto, T., Kohtz, D.S., and Lisanti, M.P. (1998) *FEBS Lett*. **428**, 205-211
8. Lee, S.W., Reimer, C.L., Oh, P., Campbell, D.B., and Schnitzer, J.E. (1998) *Oncogene* **16**, 1391-1397
9. Hurlstone, A.F., Reid, G., Reeves, J.R., Fraser, J., Strathdee, G., Rahilly, M., Parkinson, E.K., and Black, D.M. (1999) *Oncogene* **18**, 1881-1890
10. Racine, C., Belanger, M., Hirabayashi, H., Boucher, M., Chakir, J., and Couet, J. (1999) *Biochem. Biophys. Res. Commun*. **255**, 580-586
11. Galbiati, F., Volonte, D., Engelman, J.A., Watanabe, G., Burk, R., Pestell, R.G., and Lisanti, M.P. (1998) *EMBO J.* **17**, 6633-6648
12. Campbell, L., Hollins, A.J., Al-Eid, A., Newman, G.R., von Ruhland, C., and Gumbleton, M. (1999) *Biochem. Biophys. Res. Commun*. **262**, 744-751
13. Mikol, D.D., Hong, H.L., Cheng, H.L., and Feldman, E.L. (1999) *Glia* **27**, 39-52
14. Timme, T.L., Goltsov, A., Tahir, S., Li, L., Wang, J., Ren, C., Johnston, R.N, and Thompson, T.C. (2000) *Oncogene* **19**, 3256-3265
15. Li, L., Yang, G., Ebara, S., Satoh, T., Nasu, Y., Timme, T.L., Ren, C., Wang, J., Tahir, S.A., and Thompson, T.C. (2001) *Cancer Res*. **61**, 4386-4392
16. Li, L., Ren, C.H., Tahir, S.A., Ren, C., and Thompson, T.C. (2003) *Mol. Cell. Biol*. **23**, 9389-9404
17. Fiucci, G., Ravid, D., Reich, R., and Liscovitch, M. (2002) *Oncogene* **21**, 2365-2375
18. Ravid, D., Maor, S., Werner, H., and Liscovitch, M. (2005) *Oncogene* **24**, 1338-1347
19. Ho, C.C., Huang, P.H., Huang, H.Y., Chen, Y.H., Yang, P.C., and Hsu, S.M. (2002) *Am. J. Pathol*. **161**, 1647-1656
20. Liu, C.Y., Wang, C.H., and Chen, T.C. (1998) *Br. J. Cancer* **78**, 534-541
21. Arias-Diaz, J., Vara, E., and Torres-Melero, J. (1994) *Cancer* **74**, 1546-1551
22. Fujimoto, H., Ando, Y., and Yamashita, T. (1997) *Jpn. J. Cancer Res*. **88**, 1190-1198
23. Yang, G., Truong, L.D., Timme, T.L., Ren, C., Whleeler, T.M., Park, S.H., Nasu, Y., Bangma, C.H., Kattan, M.W., Scardino, P.T., and Thompson, T.C. (1998) *Clin. Cancer Res*. **4**, 1873-1880
24. Thompson, T.C. (1999) *Cancer Metastasis Rev*. **17**, 439-442
25. Thomsen, L.L., Miles, D.W., Happerfield, L., Bobrow, L.G., Knowles, R.G., and Moncada, S. (1995) *Br. J. Cancer* **72**, 41-44
26. Cobbs, C.S., Brenman, J.E., Aldape, K.D., Bredt, D.S., and Israel, M.A. (1995) *Cancer Res*. **55**, 727-730

27. Ambs, S., Merriam, W.G., Bennett, W.P., Felley-Bosco, E., Ogunfusika, M.O., Oser, S.M., Klein, S., Shields, P.G., Billiar, T.R., and Harris, C.C. (1998) *Cancer Res*. **58**, 334-341
28. Heigold, S., Sers, C., Bechtel, W., Ivanovas, B., Schafer, R., and Bauer, G. (2002) *Carcinogenesis* **23**, 929-941
29. Iyer, A.K.V., Azad, N., Wang, L., and Rojanasakul, Y. (2008) *Nitric Oxide* **19**, 146-151
30. Chanvorachote, P., Nimmannit, U., Wang, L., Stehlik, C., Lu, B., Azad, N., and Rojanasakul, Y. (2005) *J. Biol. Chem*. **280**, 42044-42050
31. Chanvorachote, P., Nimmannit, U., Stehlik, C., Wang, L., Jiang, B.H., Ongpipatanakul, B., and Rojanasakul, Y. (2006) *Cancer Res*. **66**, 6353-6360
32. Azad, N., Vallyathan, V., Wang, L., Tantishaiyakul, V., Stehlik, C., Leonard, S.S., and Rojanasakul, Y. (2006) *J. Biol. Chem*. **281**, 34124-34134
33. Ryua, S.D., Yi, H.G., Cha, Y.N., et al. (2004) *Life Sci*. **75**, 2559-2572
34. Moon, K.H., Kim, B.J., and Song, B.J. (2005) *FEBS Lett*. **579**, 6115-6120
35. Williams, T.M., Lee, H., Cheung, M.W., Cohn, A.W., Razani, B., Iyengar, P., Scherer, P.E., Pestell, R.G., and Lisanti, M.P. (2004) *J. Biol. Chem*. **279**, 24754-24756
36. Williams, T.M. and Lisanti, M.P. (2005) *Am. J. Physiol. Cell. Physiol*. **288**, 494-506
37. Hershko, A. and Ciechanover, A. (1998) *Ann. Rev. Biochem*. **67**, 425-479
38. Borutaite, V. and Brown, G.C. (2003) *Free Radic. Biol. Med*. **35**, 1457-1468
39. Souici, A.C., Mirkovitch, J., Hausel, P., Keefer, L.K., and Felley-Bosco, E. (2000) *Carcinogenesis* **21**, 281-287
40. Hess, D.T., Matsumoto, A., Kim, S.O., Marshall, H.E., and Stamler, J.S. (2005) *Nature Rev. Mol. Cell. Biol*. **6**, 150-166
41. Li, J., Billiar, T.R., Talanian, R.V., and Kim, Y.M. (1997) *Biochem. Biophys. Res. Commun*. **240**, 419-424
42. Kim, Y.M., Talanian, R.V., and Billiar, T.R. (1997) *J. Biol. Chem*. **272**, 31138-31148
43. Xu, L., Han, C., Lim, K., and Wu, T. (2008) *J. Biol. Chem*. **283**, 3077-3087

FIGURE LEGENDS

FIGURE 1. **Detachment-induced apoptosis and its inhibition by NO.** *A*, effect of cell detachment on cell survival determined by XTT assay. Lung epithelial H460 cells were detached as described in *Materials and Methods*, and suspended in HEMA-coated plated for various times (0-24 h). *B*, effect of cell detachment on apoptosis and necrosis determined by flow cytometry using annexin V-FITC (An V-FITC) and propidium iodide (PI) assays. *C*, effect of NO modulators on detachment-induced cell death. Detached cells were treated with various concentrations of NO donor, sodium nitroprusside (SNP) (10, 50, 100 μM) or diethylenetriamine (DETA) NONOate (10, 50, 100 μM), or with NO inhibitor, aminoguanidine (AG) (100, 200, 300 μM) or PTIO (10, 50, 100 μM) for 12 h. Cell survival was then determined by XTT assay. *D*, effects of NO modulators on detachment-induced apoptosis and necrosis. Detached cells were treated with SNP (50 μM), DETA NONOate (50 μM), AG (300 μM), or PTIO (50 μM) for 12 h, and cell apoptosis and necrosis were determined as described above. *E*, Upper panel, effect of NO modulators on detachment-induced apoptosis determined by Hoechst 33342 nuclear fluorescence staining. Lower panel, effect of NO modulators on detachment-induced apoptosis determined by annexin V-FITC fluorescence microscopy. Data are mean ± S.D. (n = 3). *$p <$ 0.05 *versus* non-treated control.

FIGURE 2. **Effect of NO modulators on cellular NO and nitrite levels.** H460 cells were detached and either lefted untreated or treated with SNP (50 μM), DETA NONOate (50 μM), AG (300 μM), or PTIO (50 μM) for 2 h. *A*, nitrite production determined by Griess assay. *B* and *C*, NO production determined by flow cytometry and fluorescence microscopy using DAF-DA as a probe. Data are mean ± S.D. (n = 3). *$p < 0.05$ *versus* non-treated control.

FIGURE 3. **Cav-1 overexpression increases cell death resistance, alters growth pattern, and increases growth rate.** *A*, H460 cells were stably transfected with Cav-1 or control plasmid as described in *Materials and Methods*. Transfected cells were grown in culture medium and analyzed for cell proliferation at various times using a hemocytometer. *B*, Western blot analysis of Cav-1 expression in control and Cav-1-transfected cells. Cell extracts were prepared and separated on 10% polyacrylamide-SDS gels, transferred, and probed with Cav-1 antibody. β-actin was used as a loading control. *C*, effect of cell detachment on cell survival determined by XTT assay. *D*, morphology of control and Cav-1-transfected cells in culture. Data are mean ± S.D. (n = 3). *$p < 0.05$ *versus* vector-transfected control.

FIGURE 4. **Effect of cell detachment on Cav-1 expression and its regulation by NO.** *A*, H460 cells were detached and seeded in HEMA-coated plates for various times (0-24 h) in the presence or absence of lactacystin (LAC) (10 μM). Cells extracts were prepared and analyzed for Cav-1 protein expression by Western blotting. Blots were reprobed with β-actin antibody to confirm equal loading of samples. The immunoblot signals were quantified by densitometry, and mean data from independent experiments (one of which is shown here) were normalized to the results in control cells at 0 h. *B*, RT-PCR analysis of Cav-1 and GAPDH mRNA expression at various times (0-24 h) after cell detachment as described in *Materials and Methods*. *C*, detached cells were treated with NO inhibitor, AG (300 μM) or PTIO (50 μM), or with NO donor, SNP (50 μM) or DETA NONOate (50 μM) for 12 h, after which they were analyzed for Cav-

1expression by Western blotting. Data are mean ± S.D. (n = 3). *$p < 0.05$ *versus* attached cell control; $^{\#}p < 0.05$ *versus* the indicated control or 12-h detached cell control.

FIGURE 5. **Effects of NO modulators on Cav-1 ubiquitination and *S*-nitrosylation.** *A*, H460 cells were detached and either left untreated or treated with SNP (50 μM) or DETA NONOate (50 μM) in the presence or absence of DTT (1 mM) in HEMA-coated plates. Cells lysates were prepared and immunoprecipitated with anti-Cav-1 antibody. The resulting immune complexes were then analyzed for ubiquitin by Western blotting at various times. Maximum ubiquitination of Cav-1 was observed at approximately 3 h after cell detachment. Lysate input was determined by probing β-actin. *B*, detached cells were similarly treated with the test agents and Cav-1 *S*-nitrosylation was determined by immunoprecipitation using anti-Cav-1 antibody, followed by Western blot analysis of the immunoprecipitated protein using anti-*S*-nitrosocysteine antibody. Densitometry was performed to determine the relative *S*-nitrosocysteine/β-actin levels. *C*, Cav-1 *S*-nitrosylation determined by fluorometry. Immunoprecipitates from above were incubated with 200 μM $HgCl_2$ and 200 μM diaminonaphthalene in PBS. NO released from *S*-nitrosylated Cav-1 was quantified at 375/450 nm. Plots are mean ± S.D. (n = 3). *$p < 0.05$ *versus* non-treated control; $^{\#}p < 0.05$ *versus* the indicated treatment controls.

FIGURE 6. **NO inhibits detachment-induced Cav-1 downregulation and cell death.** *A*, H460 cells were detached and either left untreated or treated with SNP (50 μM) or DETA NONOate (50 μM) in the presence or absence of DTT (1 mM) in HEMA-coated plates. *A*, cell lysates were prepared and analyzed for Cav-1 protein expression by Western blotting after 12 h. Densitometry was performed to determine the relative levels of Cav-1 after reprobing the membranes with β-actin antibody. *B*, cells survival was determined by XTT assay after 12 h. *C*, morphology of cells treated with SNP (50 μM) or DETA NONOate (50 μM) for 12 h. Data are mean ± S.D. (n = 3). *$p < 0.05$ *versus* non-treated control; $^{\#}p < 0.05$ *versus* the indicated treatment controls.

Figure 1

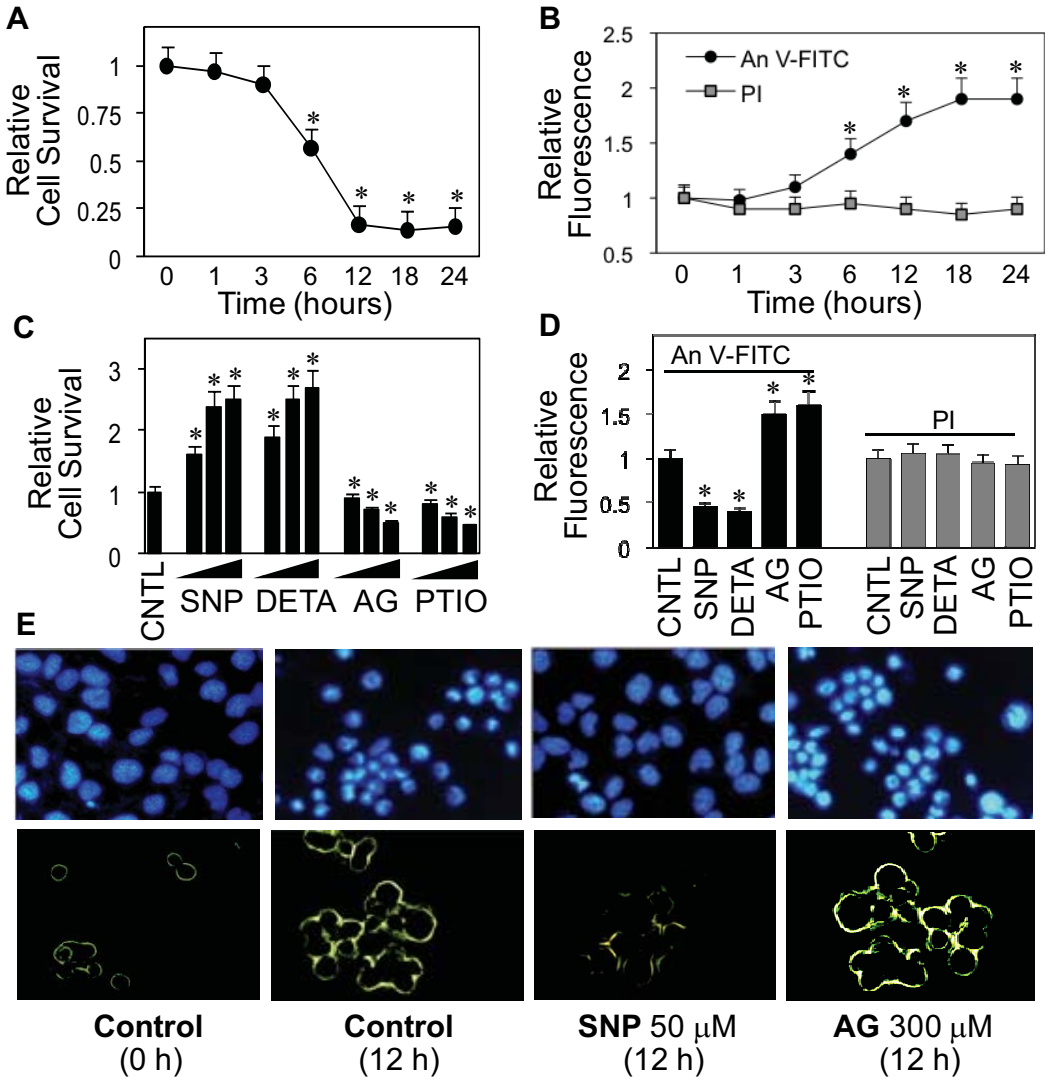
A
Relative Cell Survival
1
0.75
0.5
0.25
0
0 1 3 6 12 18 24
Time (hours)
B
Relative Fluorescence
2.5
2
1.5
1
0.5
An V-FITC
PI
0 1 3 6 12 18 24
Time (hours)
C
Relative Cell Survival
3
2
1
0
CNTL
SNP
DETA
AG
PTIO
D
Relative Fluorescence
2
1.5
1
0.5
0
An V-FITC
PI
CNTL
SNP
DETA
AG
PTIO
CNTL
SNP
DETA
AG
PTIO
E
Control (0 h)
Control (12 h)
SNP 50 μM (12 h)
AG 300 μM (12 h)

Figure 2

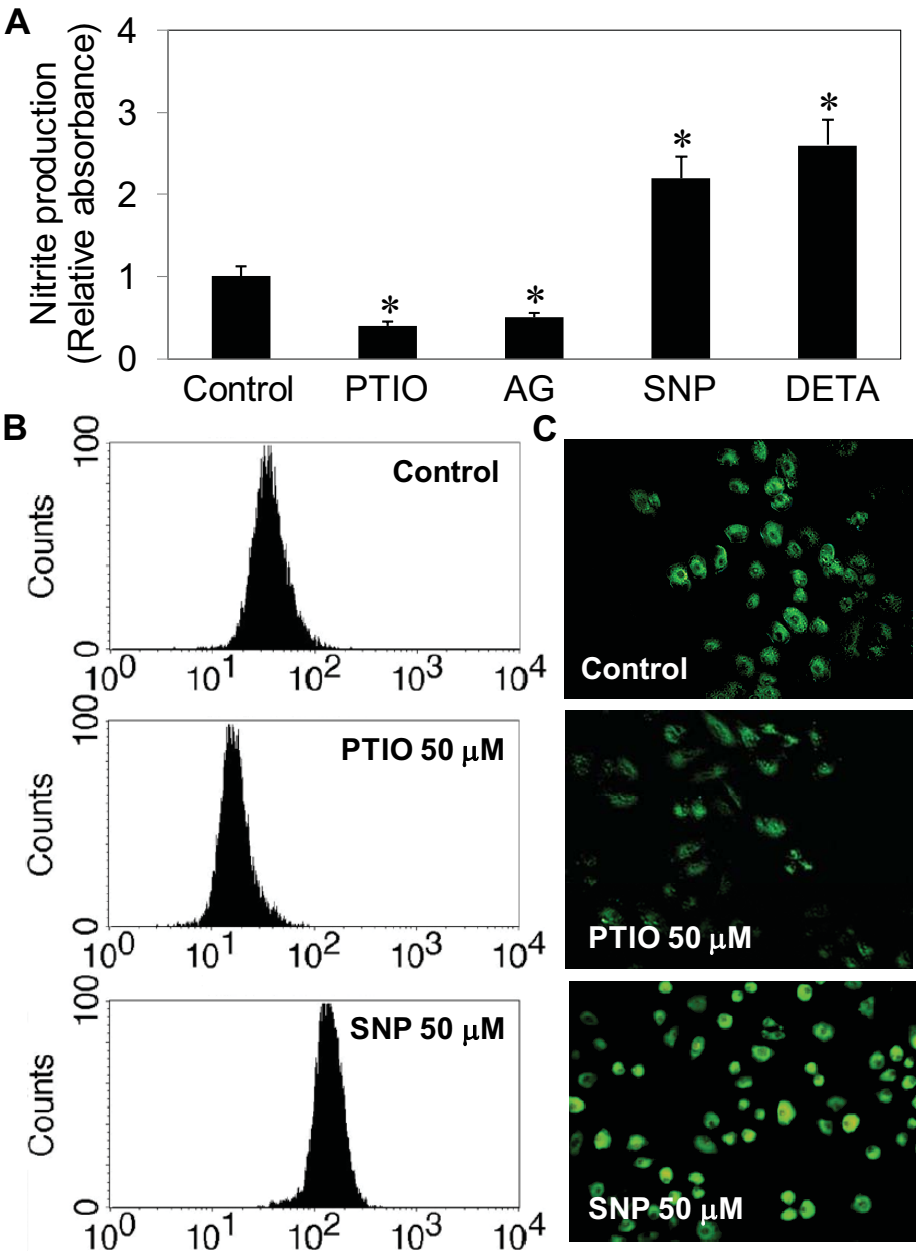
A
Nitrite production
(Relative absorbance)
4
3
2
1
0
*
*
*
*
Control
PTIO
AG
SNP
DETA
B
C
Counts
100
0
Control
PTIO 50 μM
SNP 50 μM
10^0
10^1
10^2
10^3
10^4

Figure 3

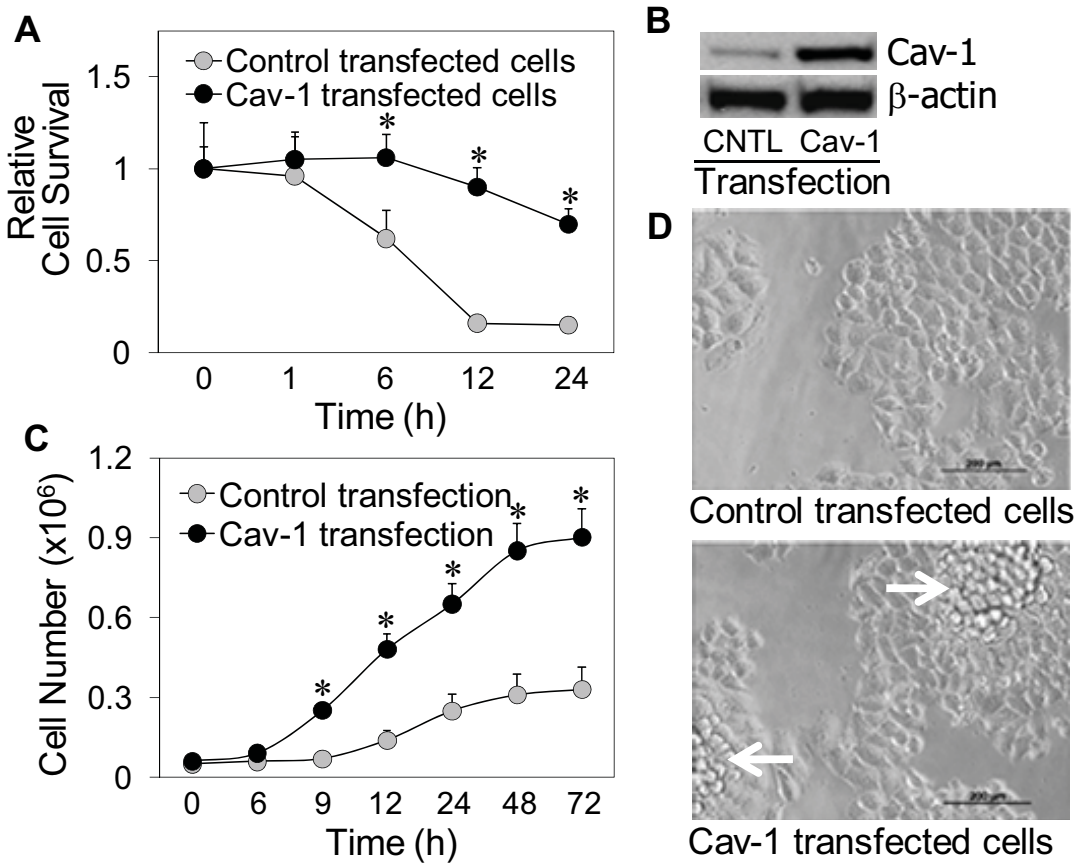
A
Relative Cell Survival
Control transfected cells
Cav-1 transfected cells
1.5
1
0.5
0
0
1
6
12
24
Time (h)
B
Cav-1
β-actin
CNTL
Cav-1
Transfection
C
Cell Number (x10^6)
Control transfection
Cav-1 transfection
1.2
0.9
0.6
0.3
0
0
6
9
12
24
48
72
Time (h)
D
Control transfected cells
Cav-1 transfected cells

Figure 4

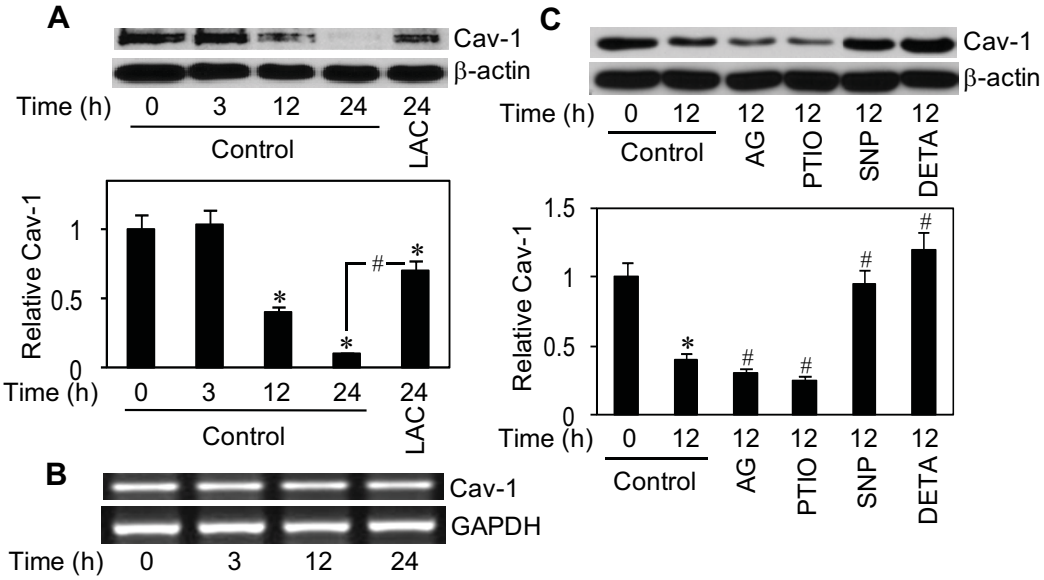
A
Cav-1
β-actin
Time (h) 0 3 12 24 24
Control
LAC
Relative Cav-1
1
0.5
0
Time (h) 0 3 12 24 24
Control
LAC
B
Cav-1
GAPDH
Time (h) 0 3 12 24
C
Cav-1
β-actin
Time (h) 0 12 12 12 12 12
Control
AG
PTIO
SNP
DETA
Relative Cav-1
1.5
1
0.5
0
Time (h) 0 12 12 12 12 12
Control
AG
PTIO
SNP
DETA

Figure 5

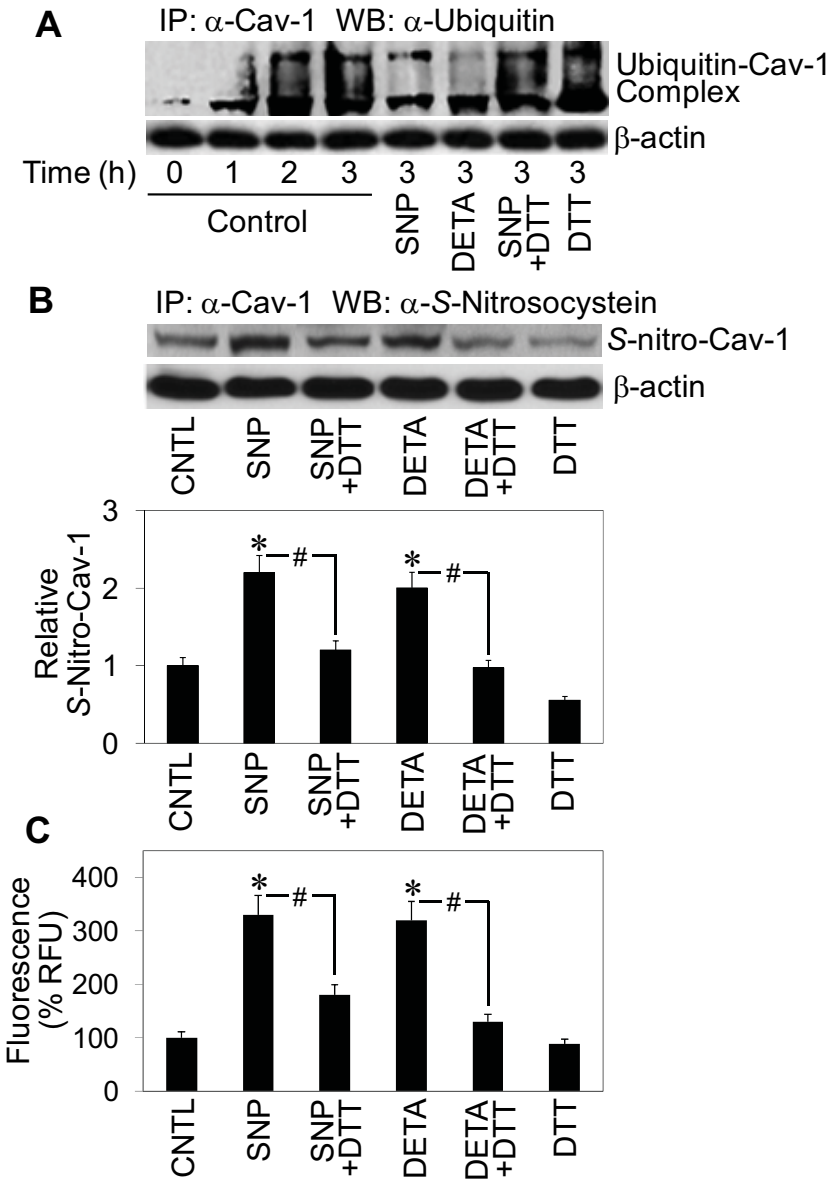
A
IP: α-Cav-1 WB: α-Ubiquitin
Ubiquitin-Cav-1 Complex
β-actin
Time (h) 0 1 2 3 3 3 3 3
Control
SNP
DETA
SNP +DTT
DTT
B
IP: α-Cav-1 WB: α-S-Nitrosocystein
S-nitro-Cav-1
β-actin
CNTL
SNP
SNP +DTT
DETA
DETA +DTT
DTT
Relative S-Nitro-Cav-1
0
1
2
3
*
#
C
Fluorescence (% RFU)
0
100
200
300
400

Figure 6

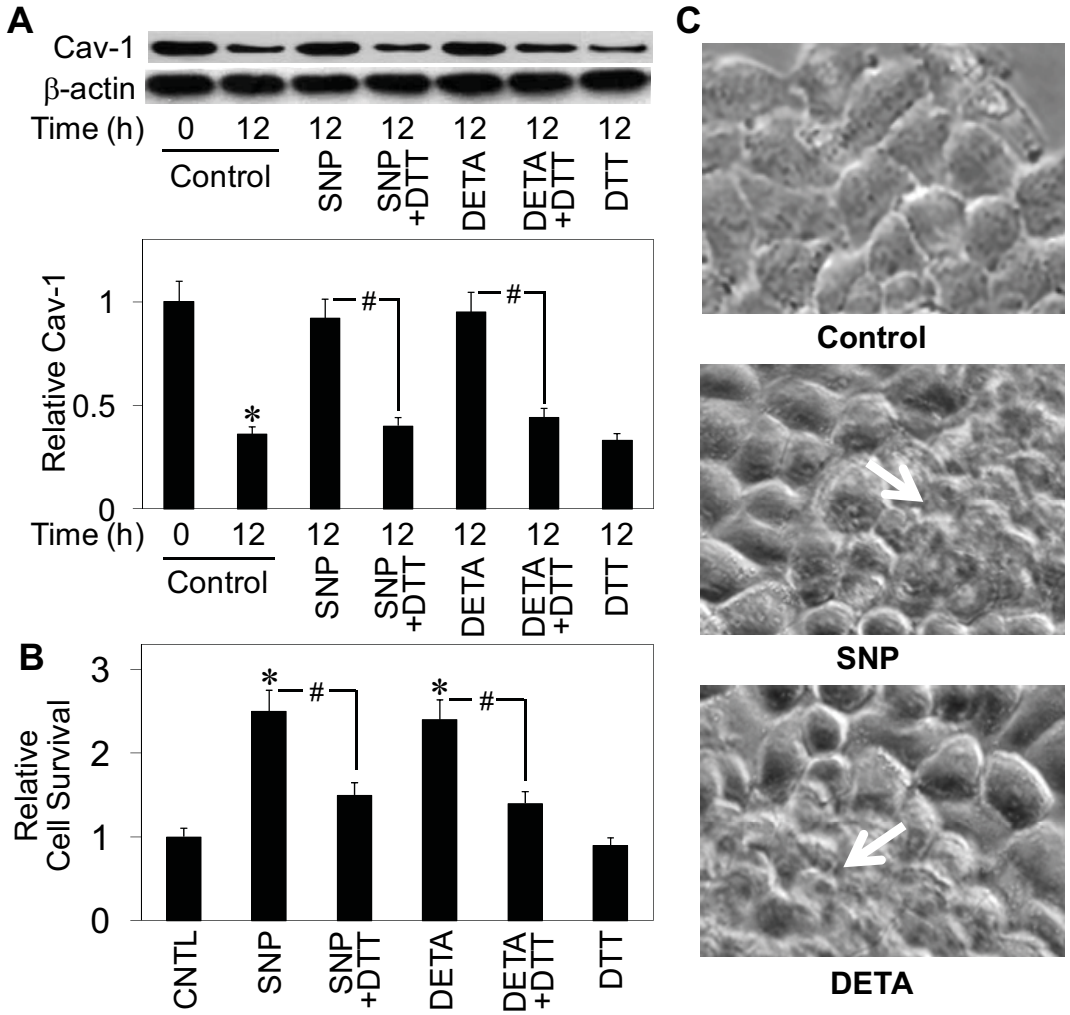
A
Cav-1
β-actin
Time (h) 0 12 12 12 12 12 12
Control
SNP
SNP +DTT
DETA
DETA +DTT
DTT
Relative Cav-1
1
0.5
0
*
#
#
Time (h) 0 12 12 12 12 12 12
Control
SNP
SNP +DTT
DETA
DETA +DTT
DTT
B
Relative Cell Survival
3
2
1
0
*
#
*
#
CNTL
SNP
SNP +DTT
DETA
DETA +DTT
DTT
C
Control
SNP
DETA

Sensitizing effect of curcumin on cisplatin-induced apoptosis involves superoxide anion induction and Bcl-2 down-regulation

Pithi Chanvorachote[1], Varisa Pongrakhananon[2], Sudjit Luanpitpong[2], Ubonthip Nimmannit[2]
[1]Department of Physiology, [2]Pharmaceutical Technology Program,
Faculty of Pharmaceutical Sciences, Chulalongkorn University, Bangkok, Thailand

Abstract

The present study reveals the sensitizing effect of curcumin on cisplatin-induced apoptosis in non-small cell lung cancer (NSCLC) cells. Curcumin induced superoxide anion generation, down-regulated anti-apoptotic Bcl-2 protein, and subsequently sensitized NSCLC H460 cells to cisplatin-induced apoptosis. The mechanism by which curcumin down-regulated Bcl-2 and sensitized cells to cisplatin-induced apoptosis involved curcumin-induced intracellular superoxide anion generation. These findings indicate a novel pathway for curcumin regulation of Bcl-2, which benefits the development of a cisplatin sensitizing agent.

Introduction

Cisplatin-based chemotherapy has been widely used for the treatment of many solid tumors including those in NSCLC. However, several studies reported that the anti-apoptotic Bcl-2 protein plays an important role in the development of cisplatin resistance in many cancer cells [1,2]. Curcumin [1,7-bis (4-hydroxy-3-methoxyphenol)-1,6-heptadiene-3,5-dione] has been reported to possesses ROS-inducing or prooxidant activity [3]. Because oxidative stress induced by cisplatin was shown to be related to cisplatin-induced apoptosis [4], prooxidant property of curcumin may be used to sensitize cancer cells to cisplatin-induced apoptosis and may increase the effectiveness of cancer treatment through combination therapy.

Materials and Methods

Cell culture and reagents

Human non small cell lung cancer (NCI-H460) cells were obtained from the American Type Culture Collection (Rockville, MD). Cells were cultured in RPMI-1640 medium containing 5% fetal bovine serum, 2 mmol/L L-glutamine, and 100 units/ml penicillin/streptomycin in a 5% CO2 environment at 37 °C.

Apoptosis and cytotoxicity assays

Apoptosis was determined by Hoechst 33342 assay. Cells were scored for the percentage of cells having intensely condensed chromatin and/or fragmented nuclei under fluorescence microscopy. Cytotoxicity was determined by MTT colorimetric assay at 550 nm.

ROS detection

Intracellular ROS generation was determined using the oxidative probe DCF-DA. Briefly, cells were incubated with the probe for 30 min at 37 °C, and analyzed for fluorescence intensity by flow cytometry.

Western blot analysis

After specific treatments, cells were lysed for 30 min on ice. Then the supernatants were collected and determined for protein content using the Bradford method. Proteins (40 µg) were resolved by 10% SDS-PAGE and transferred onto nitrocellulose membranes. The transferred membranes were blocked for 1 h in 5% nonfat milk and incubated with the anti-Bcl-2 antibodies at 4°C for 10 h. Membranes were washed and incubated with peroxidase-coupled secondary antibodies for 1 h. The immune complexes were detected by enhanced chemiluminescence detection system and quantified using analyst/PC densitometry software.

Results and Discussion

1. Cisplatin induces cell apoptosis and its sensitization by curcumin.

To investigate the role of curcumin in cisplatin-induced apoptosis, we first evaluated the dose-dependent effect of cisplatin on apoptotic cell death in H460 cells in the presence or absence of curcumin. Cisplatin treatment caused a dose-dependent increase in apoptotic cell death as compared to nontreated control (Fig. 1a). Apoptotic cells exhibited intense nuclear fluorescence, chromatin condensation and/or fragmentation. Curcumin significantly increased the apoptotic effect of cisplatin (Fig. 1a and b) indicating that curcumin enhances apoptotic cell death of cisplatin. To confirm the results, cell viability was determined by MTT assay (Fig. 1c). Previous studies have shown that curcumin can induce intracellular ROS generation which then linked to apoptotic cell death [4], we investigated whether the sensitizing effect of curcumin was associated with its ROS-inducing activity. Fig. 1a shows that addition of an anti-oxidant, N-acetyl cysteine (NAC), completely inhibited the apoptotic sensitizing effect of curcumin, suggesting that ROS was associated on this apoptotic sensitization.

2. Curcumin induces intracellular superoxide anion generation in H460 cells

Flow cytometric analysis of ROS generation using DCF-DA as a fluorescent probe shows that curcumin was able to induce ROS generation in a dose-dependent manner and that this effect was inhibited by the antioxidant NAC (Fig. 2). To determine specific ROS induced by curcumin, cells were treated with the agent in the presence or absence of various known specific antioxidants, including MnTBAP (a superoxide dismutase mimetic and scavenger of superoxide anion), catalase (hydrogen peroxide scavenger), and sodium formate (hydroxyl radical scavenger). Cells were then analyzed for ROS as described. The results show that MnTBAP significantly inhibited curcumin-induced ROS generation, whereas other antioxidants had no significant effect (Fig. 2). These findings indicate that superoxide anion is a major ROS induced by curcumin in the treated cells.

3. Curcumin promotes down-regulation of Bcl-2 by cisplatin through an ROS-dependent mechanism

Overexpression of Bcl-2 has also been associated with cisplatin resistance in many cell types [1,2]. To test whether curcumin might promote cisplatin-induced cell death through down-regulation of Bcl-2, we analyzed Bcl-2 expression levels in cells treated with curcumin and cisplatin by Western blotting. Fig. 3 shows that cisplatin induced a dose-dependent decrease in Bcl-2 expression and addition of curcumin further decreased the Bcl-2 expression. Co-treatment of the cells with antioxidant NAC inhibited this down-regulation, indicating the requirement of ROS in the process.

4. Superoxide-mediated down-regulation of Bcl-2 by curcumin

Curcumin was earlier shown to promote Bcl-2 down-regulation by cisplatin in an ROS-dependent manner; we next determined whether curcumin can directly induce Bcl-2 down-regulation and, if so, what specific ROS are involved. Cells were treated with various concentrations of curcumin and its effect on Bcl-2 expression was determined. The result shows that curcumin could directly induce Bcl-2 down-regulation in dose-dependent manner and this effect is completely inhibited by the antioxidant NAC (Fig. 4). To determine the specific ROS involved, cells were treated with curcumin in the presence or absence of specific ROS scavengers, including MnTBAP, catalase, deferoxamine, and sodium formate; and their effect on Bcl-2 expression was determined. Fig. 4 shows that the superoxide dismutase scavenger MnTBAP completely inhibited curcumin-induced Bcl-2 down-regulation, whereas other antioxidants had no significant inhibitory effect. These results indicate that superoxide anion is the primary ROS responsible for the curcumin induction of Bcl-2 down-regulation.

Fig. 1.

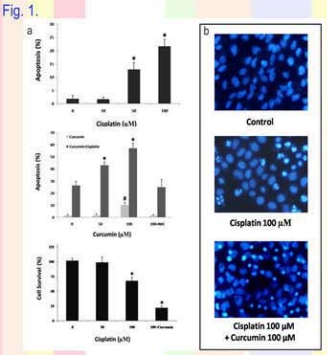

Fig. 2.

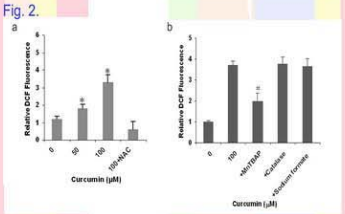

Fig. 3.

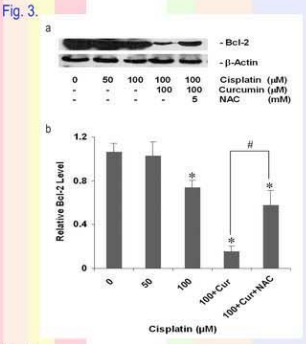

Fig. 4.

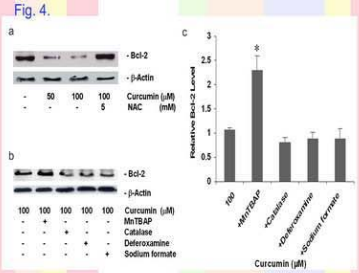

Acknowledgement

This research was supported by the Thailand Research Fund (MRG G5080134), and Grant for development of new staff, Chulalongkorn University.

References

1. *Oncogene* 1998; 19: 933-943.
2. *Cancer Res. Clin. Oncol.* 2004; 130: 423-428.
3. *Toxicol. In Vitro.* 2004; 18: 783-789.
4. *Int. J. Oncol.* 2004; 25: 1671-1676.